Dynamic interpretation of slug tests in highly permeable aquifers

Brian R. Zurbuchen and Vitaly A. Zlotnik
Department of Geosciences, University of Nebraska, Lincoln, Nebraska, USA

James J. Butler Jr.
Kansas Geological Survey, University of Kansas, Lawrence, Kansas, USA

Received 19 September 2000; revised 15 January 2001; accepted 3 October 2001; published 21 March 2002.

[1] Considerable progress has been made in developing a theoretical framework for modeling slug test responses in formations with high hydraulic conductivity K. However, several questions of practical significance remain unresolved. Given the rapid and often oscillatory nature of test responses, the traditional hydrostatic relationship between the water level and the transducer-measured head in the water column may not be appropriate. A general dynamic interpretation is proposed that describes the relationship between water level response and transducer-measured head. This theory is utilized to develop a procedure for transforming model-generated water level responses to transducer readings. The magnitude of the difference between the actual water level position and the apparent position based on the transducer measurement is a function of the acceleration and velocity of the water column, test geometry, and depth of the transducer. The dynamic approach explains the entire slug test response, including the often-noted discrepancy between the actual initial water level displacement and that measured by a transducer in the water column. Failure to use this approach can lead to a significant underestimation of K when the transducer is a considerable distance below the static water level. Previous investigators have noted a dependence of test responses on the magnitude of the initial water level displacement and have developed various approximate methods for analyzing such data. These methods are re-examined and their limitations clarified. Practical field guidelines are proposed on the basis of findings of this work. The soundness of the dynamic approach is demonstrated through a comparison of K profiles from a series of multilevel slug tests with those from dipole-flow tests performed in the same wells. *INDEX TERMS:* 1829 Hydrology: Groundwater Hydrology; 1894 Hydrology: Instruments and Techniques; 1832 Hydrology: Groundwater Transport; *KEYWORDS:* hydraulic conductivity, underdamped, transducer, initial displacement, pneumatic, dipole-flow test

1. Introduction

[2] The slug test is a commonly used field method for obtaining estimates of the hydraulic conductivity K of the portion of the formation in the vicinity of a test well. Although this technique has received increased attention in recent years as a result of the need to characterize spatial variations in K for contaminant transport investigations, there are still many unresolved issues regarding the approach [*Butler*, 1997]. One area in which there are a large number of outstanding questions is that of slug tests in highly permeable aquifers; an in-depth investigation of which is the subject of this article.

[3] The primary focus of this article will be on slug tests in partially penetrating wells in highly permeable aquifers. This topic is of considerable practical relevance because a partially penetrating well configuration (Figure 1a) is appropriate for most slug tests performed in conventional monitoring wells, where the length of the screen is short relative to the aquifer thickness. A similar configuration is the multilevel slug test (MLST), where isolated short sections of a longer well screen essentially serve as partially penetrating wells (Figure 1b). In that case, packers isolate a short section of well screen, and a riser pipe extends from the top packer to the surface. Regardless of whether a slug test is performed in a conventional (Figure 1a) or multilevel (Figure 1b) format, the pneumatic method [*Prosser*, 1981] is most appropriate for test initiation in highly permeable intervals (see Appendix A). Given the short duration of slug tests in highly permeable aquifers, a pressure transducer, positioned in the casing or riser pipe, is commonly used to indirectly monitor the response of the water level.

[4] The water level response to slug tests in highly permeable aquifers is typically very rapid and oscillatory [*Bredehoeft et al.*, 1966; *van der Kamp*, 1976; *Kipp*, 1985; *Kabala et al.*, 1985; *Springer and Gelhar*, 1991; *McElwee and Zenner*, 1998; *Zlotnik and McGuire*, 1998a]. Velocities and acceleration can be on the order of $\approx$1 m/s and $\approx$1 m/s^2, respectively. The complex hydrodynamic processes associated with slug tests in such conditions include groundwater flow and exchange with the well, momentum dynamics of the water column in the casing or riser pipe, major losses due to friction, minor losses due to contractions and expansions of the casing or riser pipe, head losses through the screen, and turbulent head losses in the aquifer. Several recent contributions [e.g., *Springer and Gelhar*, 1991; *McElwee and Zenner*, 1998; *Zlotnik and McGuire*, 1998a, 1998b] have highlighted the phenomena that must be considered when extending slug test methodology to this hydrologic setting, but a general framework that considers all relevant mechanisms has yet to be defined.

[5] The neglect of these additional mechanisms affecting slug tests in highly permeable aquifers can have significant practical ramifications. For example, as stated earlier, a submersible pressure transducer is commonly used for the indirect measurement of the water level response during a slug test. For slug tests in formations of moderate to low permeability the transducer readings of head h_{Tz}

0043-1397/02/2001WR000354

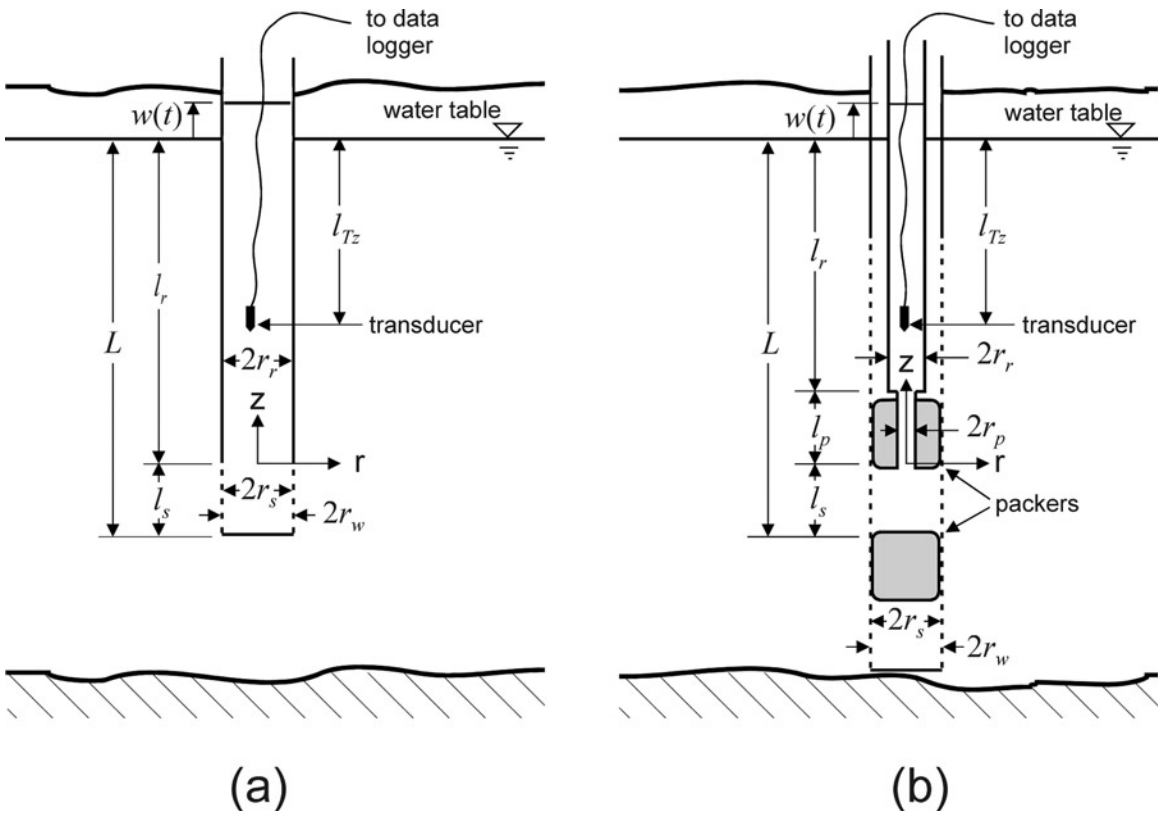

Figure 1. Schematic of (a) slug test performed in partially penetrating well and (b) multilevel slug test. Although not shown, depth to transducer positioned within the screened interval between packers is designated as l_{Ts}.

at depth l_{Tz} below the static water level are translated to water level response by assuming a hydrostatic distribution of head. However, in highly permeable aquifers the aforementioned hydrodynamic processes modify the functional relationship between transducer readings and water level. Therefore commonly used methods for interpretation of transducer readings may no longer be appropriate.

[6] Experimental data from a shallow, unconfined alluvial aquifer can be used to illustrate the dependence on transducer position that arises as a result of these complex hydrodynamic processes. The two series of slug tests presented in Figure 2 clearly illustrate that the transducer-measured response is dependent on the depth of the transducer in the water column. Figure 2a presents results from slug tests in a single monitoring well, while Figure 2b presents results from a set of MLSTs performed in an isolated short section of a longer screened well. In both cases, tests were initiated pneumatically, and all test parameters, with the exception of l_{Tz}, remained unchanged between tests.

[7] It is apparent from Figure 2 that as the transducer is positioned deeper in the water column, the traditional assumption of hydrostatic head distribution in the water column (i.e., the assumption that the transducer-measured head is reflective of the water level) becomes increasingly inappropriate. Three features are of particular interest. First, in the initial portions of the test, there is a significant difference between the initial head change measured by the transducer and the actual initial displacement. Previously, these differences were attributed to noninstantaneous air evacuation [e.g., *Prosser*, 1981, p. 590; *Butler et al.*, 1996, Figure 6] or instrument problems. Second, the response data become increasingly damped and shifted in phase as the transducer is positioned at greater depth in the water column. Third, there are perturbations present in the initial portion of the data [see also *Butler et al.*, 1996, Figure 6]. These perturbations, which rapidly decay, have a magnitude that is slightly negatively correlated with depth of the transducer. Although these features may be absent for the slower water column responses associated with slug tests in media of moderate to low K, they must be considered when designing a slug test (or any other type of single-well hydraulic test) in formations of high K. The appropriateness of ad hoc approaches for approximate consideration of these conditions [e.g., *Butler*, 1997, Figure 8.1; *Zlotnik and McGuire*, 1998b] must be assessed on a test-by-test basis.

[8] Another example of the complex hydrodynamic conditions associated with slug tests in highly permeable aquifers is shown in Figure 3, where normalized test responses, recorded by a transducer positioned in the tested screen section, display a nonlinear dependence on the magnitude of the initial water level displacement w_0 for $w_0 \geq 0.265$ m. This dependence is often seen in slug tests in highly permeable aquifers [e.g., *Butler et al.*, 1996; *McElwee and Zenner*, 1998]. In this case, conventional interpretation methods could produce an error in the K estimate exceeding a factor of 4. *McElwee and Zenner* [1998] proposed a model that incorporated possible mechanisms responsible for this dependence. Other investigators [*van der Kamp*, 1976, p. 72; *Kipp*, 1985, p. 1398; *Butler*, 1997, p. 167] have recommended that tests be initiated with very small initial displacements to minimize the significance of this dependence and to yield consistent estimates of K.

[9] The investigation of these complex hydrodynamic conditions and their practical ramifications is the major purpose of this article. Our goal is to develop a theoretical foundation for slug tests in highly permeable aquifers and to use this as the basis for the definition of a series of practical guidelines for the acquisition and interpretation of slug test data in this important hydrogeologic setting.

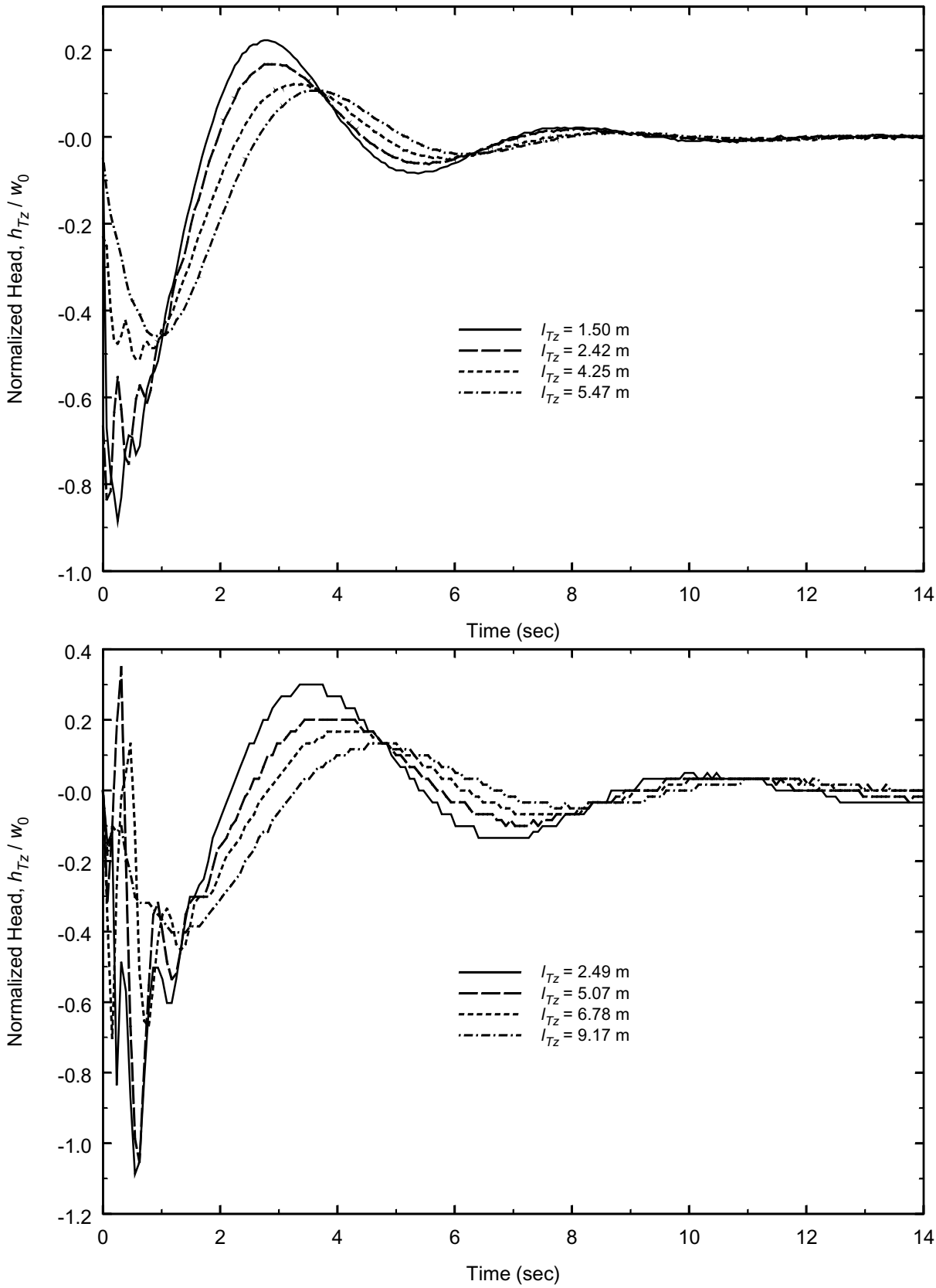

Figure 2. Normalized transducer-recorded head responses from two series of slug tests in the alluvial aquifer of the Platte River, Nebraska. (a) Responses from partially penetrating well C6i at the Silvercreek field site. (b) Responses from multilevel slug tests (MLSTs) in well 15 (depth of tested interval 13.4 m) at the Management Systems Evaluation Area (MSEA) site. Head responses recorded with transducer positioned at different depths in the water column l_{Tz}. Slug test specifications are $w_0 = 0.192$ m, $l_s = 0.76$ m, $l_r = 5.65$ m, $r_w = 3.0$ cm, and $r_r = r_s = 2.6$ cm. MLST specifications are $w_0 = 0.265$ m, $l_s = 0.82$ m, $l_p = 0.63$ m, $l_r = 8.65$ m, $r_w = 5.7$ cm, $r_s = 5.1$ cm, $r_p = 1.9$ cm, and $r_r = 2.5$ cm.

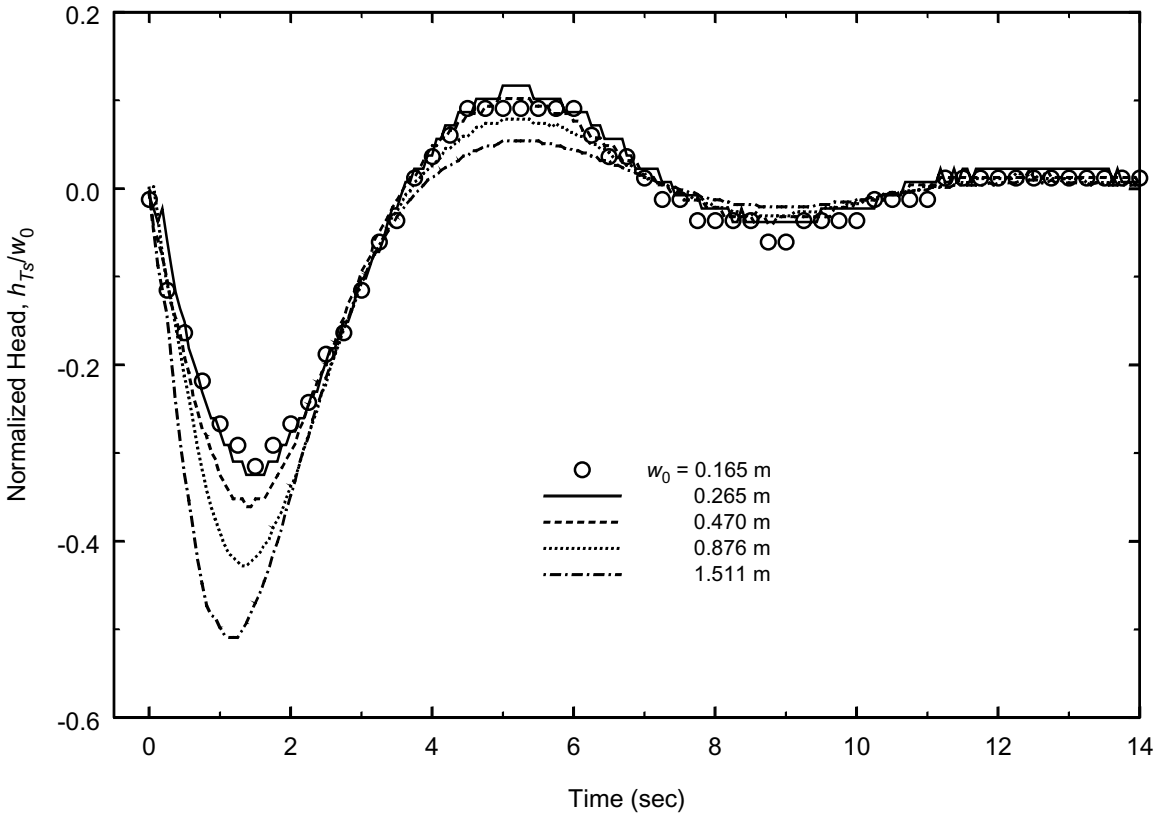

Figure 3. Normalized head responses obtained in well 15 (depth of tested interval 14.3 m) using various initial displacements. Pressure response for small w_0 (0.165 and 0.265 m) illustrate approximately linear behavior. MLST specifications are the same as in Figure 2b with the exceptions l_{Ts} = 10.9 m, l_s = 0.62 m, and l_r = 9.65 m. Note that symbols are displayed at 1/4 of the field-recorded frequency.

[10] This article will begin with a review of well hydraulics for slug tests in highly permeable aquifers. The multilevel slug test configuration of Figure 1b will be the focus of the discussion in order to maximize the generality of the presentation. The relationship between water level response and transducer-measured head will then be discussed, and a correction formula that accounts for the position of the transducer in the water column will be derived. This formula, which can be used to transform model-generated water levels into transducer-measured head, will be incorporated into a new dynamic method for data interpretation. This dynamic method will be illustrated using multilevel slug test data from a well-characterized field site. The advantages of the proposed dynamic method will be shown by comparison to results obtained using previously proposed approaches for data interpretation. The validity of the dynamic method will be demonstrated through comparison with *K* profiles obtained at the same wells using the dipole-flow test [*Zlotnik and Zurbuchen*, 1998]. Finally, the practical findings of this work will be summarized in a set of field guidelines.

2. Theory

2.1. Generalized Model of Flow in the Well

[11] Development of a model of the complex hydrodynamic conditions during a slug test in a highly permeable aquifer requires consideration of the following physical processes and factors: (1) the minor head losses due to pipe contractions and enlargements; (2) the flow regime (laminar, turbulent, or transitory) and velocity distribution within the well and portion of aquifer near the screen and associated major head losses; (3) the spatial (vertical) distribution of mass flux across the well screen; and (4) the slug test initiation method (e.g., solid slug or pneumatic). Since most of these processes cannot be described from first principles, any model will be limited in rigor and accuracy. Therefore two approaches are feasible. The first approach is to consider the major hydraulic factors, which must be established by controlled laboratory experimentation for each test configuration. The second approach is to develop a semiempirical model of a general form in which hydraulic parameters are estimated by matching to field data. To our knowledge, efforts to investigate slug test instrumentation in controlled laboratory conditions have not been reported. All previously developed slug test models have taken the second approach. We will review these models in the following paragraphs.

[12] Three models have been developed and applied for the interpretation of oscillatory slug test responses in partially penetrating wells: the Springer-Gelhar (SG) model [*Springer and Gelhar*, 1991], the modified Springer-Gelhar (MSG) model [*Zlotnik and McGuire*, 1998a] and the McElwee-Zenner (MZ) model [*McElwee and Zenner*, 1998]. Each model was derived through application of the principles of mass and momentum conservation [e.g., *Kipp*, 1985]. All three models can be summarized using the following general differential equation relating the motion of the water level to the deviation of head at the well screen and to the air pressure above the water column:

$$(L_e + w)w'' + A_l \cdot (w')^2 + gw = gh_{Ts} - p_{\text{air}}/\rho, \qquad (1)$$

where $w(t)$ is deviation of water level from static (positive upward), $w'(t)$ and $w''(t)$ are velocity and acceleration of water level in the riser

pipe, respectively, $p_{air}(t)$ is gauge air pressure within the riser pipe (taken as $p_{air}(t) = 0$ for instantaneous release of air), the constant L_e is the effective length of the water column, A_l is an empirical coefficient (function of w and w') that accounts for various head losses in the well and aquifer, ρ is density of water, g is the gravitational constant ($g = 9.81$ m/s^2), and $h_{Ts}(t)$ is the deviation of head at the well screen $h_s(t)$ from the static head (h_0), i.e., $h_{Ts} = h_s(t) - h_0$. The three terms on the left-hand side correspond to water column momentum change, losses due to friction, and gravity effects, respectively. The two terms on the right-hand side correspond to water exchange between the well and aquifer and pressure changes at the water surface, respectively. The major differences between the three models are the degree of detail in their consideration of the hydrodynamic processes and their interpretation of L_e and A_l.

2.2. Coefficients L_e and A_l

[13] The SG, MSG, and MZ models each interpret L_e and A_l from a slightly different perspective, but all three models assume a uniform distribution of flux across the well screen and a hydrostatic distribution of head along the well screen as suggested by *Bredehoeft et al.* [1966] and *Kipp* [1985]. L_e is a function of the geometry of the screen, casing, packer, and riser pipe system. The coefficient A_l is an empirical function of w and V (where V is the average cross-sectional velocity in the pipe) that accounts for major and minor frictional losses within the well-packer-riser-pipe system and non-Darcian flow in the aquifer. Assessment of A_l is complicated by the fact that the functional form is dependent on flow direction and regime. For high velocity flow, $|A_l|$ can be approximated by a constant, while for low velocities the magnitude of the quadratic term $A_l \times (w')^2$ is small and can generally be neglected [*van der Kamp*, 1976; *Kipp*, 1985; *McElwee and Zenner*, 1998; *Zlotnik and McGuire*, 1998a]. However, due to the wide range of velocities observed in oscillatory slug tests, neither the assumption of a constant $|A_l|$ nor the neglect of the quadratic term is appropriate.

[14] To discuss the differences between the models, let us introduce l_r, l_p, l_s, r_r, r_p, and r_s as the lengths l and radii r of the riser pipe, packer pipe, and screen, respectively (Figure 1), and $L = l_r + l_p + l_s$. *Springer and Gelhar* [1991] considered the simplest slug test geometry, a well with a short screen as shown in Figure 1a, where both casing and screen have the same diameter (i.e., $r_s = r_r$). Their model disregarded major losses and excluded minor losses since neither contractions nor expansions were present. Equation (1) was linearized by assuming

$$L_e + w \approx L_e = l_r + \frac{l_s}{2}, \quad A_l = 0. \tag{2}$$

[15] *Zlotnik and McGuire* [1998a] modified the SG model to account for the typical configuration of the MLST (Figure 1b). This approach yielded an L_e parameter that incorporates the momentum change due to contractions and expansions in the MLST system

$$L_e = l_r + l_p \frac{r_r^2}{r_p^2} + \frac{l_s}{2}\frac{r_r^2}{r_s^2} \ . \tag{3}$$

They also considered minor losses associated with contractions and expansions. With inclusion of major losses in the riser pipe and packer assembly their coefficient $A_l(w,V)$ can be written as the sum of minor ς and major losses ψ.

$$A_l(w, V) = \frac{1}{2}\varsigma(V) + \psi(w, V) \tag{4}$$

The values of ς and ψ are velocity-dependent coefficients that can be derived from general pipe flow theory (Appendix B). The MSG model reduces to the SG model when the geometry is for a slug test in a partially penetrating well, frictional losses are neglected (i.e., $A_l = 0$), and $w_0 \ll L_e$.

[16] *McElwee and Zenner* [1998] listed the major hydraulic processes in the well, screen, and aquifer that affect L_e and $|A_l|$. Their analysis indicated that L_e and $|A_l|$ cannot be calculated from first principles. Therefore they abandoned the idea of estimating L_e and $|A_l|$ a priori and proposed a pragmatic approach to identify these parameters from field data by matching observed and theoretical responses. It was assumed that the uncertainty in L_e can be accounted for by some unknown constant β. Minor and major frictional losses and effects of non-Darcian flow in the aquifer were approximated by a constant parameter A. The resulting parameters are

$$L_e = L + \beta, \qquad A_l(w, V) = A \ \mathrm{sgn}(V) \ . \tag{5}$$

This approach of modifying L_e and A simplifies the inclusion of head losses although it limits further generalization of (1), as will be discussed later.

2.3. Aquifer Hydraulics

[17] The quasisteady model of well-aquifer interaction [*Hvorslev*, 1951; *Bouwer and Rice*, 1976] has proven to be remarkably valid for a wide range of parameters [see *Widdowson et al.*, 1990; *Hyder and Butler*, 1995; *Brown et al.*, 1995]. *Springer and Gelhar* [1991] and *McElwee and Zenner* [1998] independently proposed use of the quasisteady model to describe well-aquifer interaction in highly permeable aquifers. This model neglects aquifer compressibility and therefore assumes that the diffusivity of the aquifer is so high that changes in head at the well screen h_s are instantaneously propagated throughout the aquifer. The deviation of head at the well screen from static conditions h_{Ts} thus instantaneously invokes discharge Q to the well, which can be defined as

$$h_{Ts} = h_s(t) - h_0 = \frac{-Q}{2\pi K_r P l_s}, \quad P = P\left(\frac{r_w}{a\, l_s}, \frac{L}{l_s}, \frac{b}{l_s}\right) , \tag{6}$$

where P is a shape factor that depends on well radius r_w, aquifer thickness b, anisotropy ($a = (K_r/K_z)^{1/2}$, where K_r and K_z are horizontal and vertical hydraulic conductivity, respectively), screen length l_s, and depth from top of aquifer to base of tested screen section L [*Dagan*, 1978; *Zlotnik*, 1994].

[18] The shape factor in the quasisteady model is a function of anisotropy, which is generally not known a priori. Treatment of this factor can be based on two premises. First, all single-borehole tests are weakly sensitive to anisotropy [*Streltsova*, 1988, p. 20; *Butler*, 1997, p. 97]. Second, there is strong evidence that many aquifers of sedimentary origin exhibit a small mean local anisotropy (i.e., $a \approx 1$) [*Burger and Belitz*, 1997; *Corbett et al.*, 1998]. *Zlotnik* [1994] and *Butler* [1997, p. 89] demonstrated that consideration of anisotropy ($a > 1$) for interpretation of slug tests only slightly increases K_r. Therefore the shape factor is evaluated under the assumption of local isotropy (i.e., $a = 1$) as suggested by *Bouwer* [1996]. We estimate the shape factor from the polynomial interpretation of the *Bouwer and Rice* [1976] graphs given by *Van Rooy* [1988] (see details given by *Butler* [1997, p. 109]). Shape factor estimates can be refined

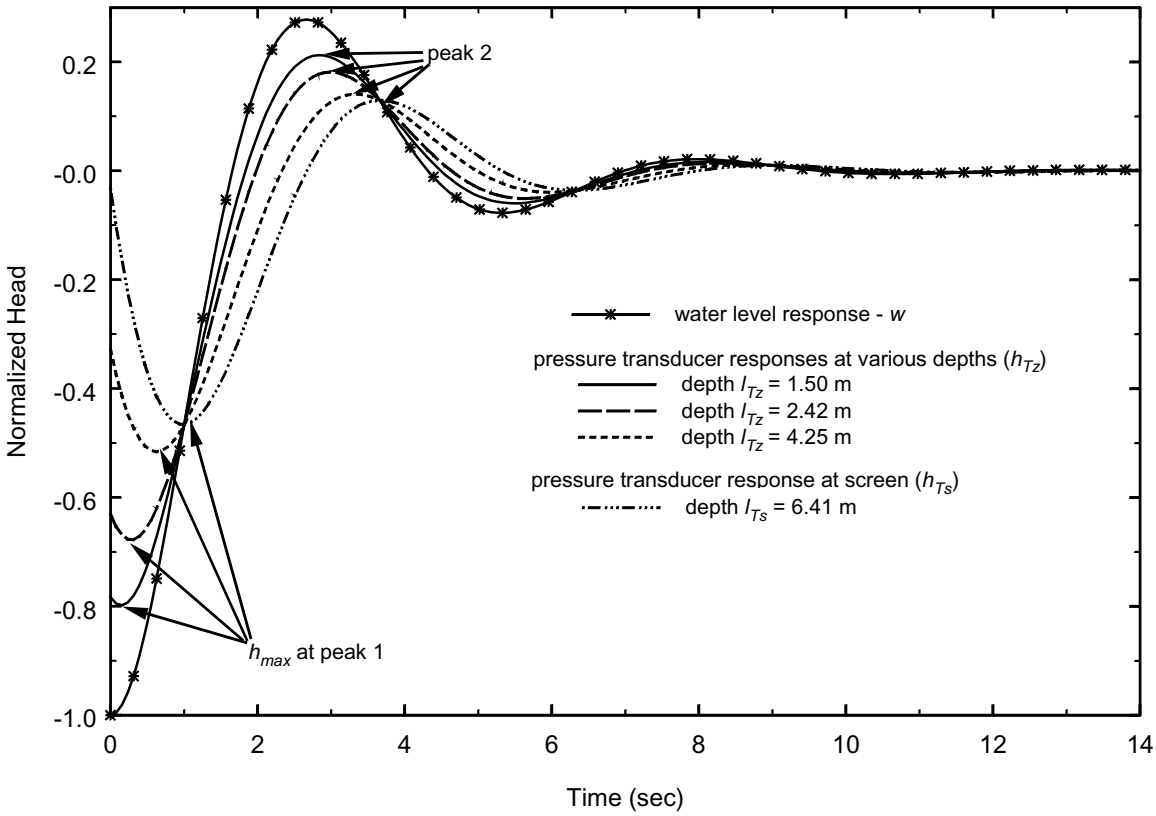

Figure 4. Simulated water level and head responses for a slug test. Aquifer parameters are $K_r = K_z = 166$ m/d. Slug test specifications are the same as in Figure 2a.

if appropriate data on anisotropy are available for the site [*Zlotnik*, 1994].

2.4. Generalized Slug Test Model: Combining Flow in Well and Aquifer

[19] Combining (1) and (6) and applying conservation of mass in the well

$$Q = \pi r_r^2 w' \tag{7}$$

yields the final general equation for the slug test:

$$(L_e + w)w'' + A_l \cdot (w')^2 + B \cdot g \cdot w' + g \cdot w = -p_{\text{air}}/\rho, \tag{8}$$

where

$$B = \frac{r_r^2}{2\, K_r\, P\, l_s}. \tag{9}$$

The initial value problem for the water level in the well is complete if one knows the initial displacement $w(0)$ and velocity $w'(0)$. Most commonly,

$$w(0) = \pm w_0, \quad w'(0) = 0, \tag{10}$$

where w_0 is the magnitude of the initial displacement and plus and minus indicate a falling or rising head test, respectively. The initial value problem of (8)–(10) for $w(t)$ can be solved using the 4th-order Runga-Kutta technique [*Press et al.*, 1989].

[20] This general model for simulation of the water level response $w(t)$ is based on mass and momentum conservation with major and minor losses and a quasisteady approximation of the well-aquifer water exchange. The model describes both monotonic (overdamped) and oscillatory (underdamped) water level responses and includes only two aquifer parameters, the horizontal hydraulic conductivity K_r and the anisotropy coefficient a. The SG, MSG, and MZ models are variations of this general model that differ in their interpretation of coefficients L_e and A_l. For the SG and MSG models the only unknown parameter is K_r if isotropy is assumed. For the MZ model, empirical parameters β and A are also unknown.

[21] On the basis of a large body of experimental data we assume instantaneously initiated slug tests ($p_{\text{air}}(t) \equiv 0$) for the remainder of this manuscript. The reader is referred to Appendix A for a detailed discussion of the dynamics of the air release process.

2.5. Generalized Slug Test Model in Dimensionless Form

[22] Introducing the dimensionless parameters

$$\tau = t\left(\frac{g}{L_e}\right)^{1/2}, \quad \overline{w} = \frac{w}{w_0}, \quad \overline{w}' = \frac{d\overline{w}}{d\tau} \tag{11}$$

yields the general dimensionless model for the water level response to a slug test

$$\overline{w}'' + F \cdot \overline{w}' + H \cdot \overline{w} = -G \cdot (\overline{w}')^2, \quad \overline{w}(0) = \pm 1, \quad \overline{w}'(0) = 0, \tag{12}$$

where

$$H(\overline{w}) = \frac{1}{(1+\overline{w}w_0/L_e)}, \quad F(\overline{w}) = F_0 \cdot H(\overline{w}),$$
$$F_0 = B \cdot (g/L_e)^{1/2}, \quad G(\overline{w}, \overline{w}') = \frac{A_l \cdot w_0}{L_e} H(\overline{w}) \tag{13}$$

and L_e and A_l are defined by either (2), (3) and (4), or (5). Similarly, the head response at the well screen given by (1) can be made dimensionless.

$$\overline{h}_{Ts} = \overline{w} + \frac{G}{H} \cdot (\overline{w}')^2 + \frac{1}{H} \cdot \overline{w}'', \qquad \overline{h}_{Ts} = \frac{h_{Ts}}{w_0} \tag{14}$$

3. Dynamic Interpretation of Transducer Response

[23] The water level recovery during slug tests in highly permeable aquifers is rapid and thus requires the use of a pressure transducer and a data logger. The slug test model presented in (8)–(10) is written in terms of water level response $w(t)$. When positioned in a static or slowly moving water column, pressure transducers can be used to calculate the position of the water level from the static pressure head at the transducer and the elevation of the transducer. However, in an accelerating water column this approach cannot be used due to the presence of a head gradient; a phenomenon that, in the context of slug tests, was first described by *Springer* [1991].

[24] In this section we derive a relationship between water level and transducer-measured head and present a new dynamic interpretation of slug test data. The derived relationship allows one to transform the model-generated water level response to the head response for a transducer positioned at any specific depth in the water column. The modeled head response is then compared to the field-measured head response for estimation of aquifer parameters. In addition, we will present a comprehensive analysis of the ramifications of equating the transducer-measured head to the modeled water level response.

[25] Equation (1) is the explicit relationship between the water level $w(t)$ and the head $h_{Ts}(t)$ that would be measured by a transducer positioned within the screened interval during a slug test. This relationship is model specific (SG, MSG, or MZ) since it is dependent on the parameters L_e and A_l. The effect of positioning the transducer at the well screen is illustrated in Figure 4 using a simulated water level response from a rising head slug test having a configuration and initial displacement w_0 identical to that used for the slug tests displayed in Figure 2a. Coefficients L_e and A_l were calculated with (2) according to the SG method, which assumes small initial displacements ($w_0/L_e \ll 1$). Using the analytical solution employed by *Springer and Gelhar* [1991], the water level response $w(t)$ was calculated and is shown in normalized form $\overline{w}(t)$ in Figure 4. The head response at the screen $h_{Ts}(t)$ was obtained by analytically calculating w' and w'' and by substituting into (1). The divergence of $\overline{w}(t)$ and $\overline{h}_{Ts}(t)$ in magnitude and phase is obvious.

[26] In practice, it is customary to position the pressure transducer at a depth l_{Tz} below the static water level in the riser pipe ($w_0 < l_{Tz} < l_r$). In this case, (1) does not describe the head response at the transducer. An expression relating the water level $w(t)$ and the deviation of head at depth l_{Tz} from static conditions ($h_{Tz}(t) = h_z(t) - h_0$) can be derived by applying conservation of mass and momentum principles [see *Kipp*, 1985]. Using Figure 1, we can define a control volume inside the riser pipe between the elevation of the transducer $z = l_r + l_p - l_{Tz}$ and the moving water level $z = l_r + l_p + w(t)$ (where $l_p = 0$ for Figure 1a and $l_p > 0$ for Figure 1b). The momentum conservation equation for this volume is:

$$p_{Tz} - (l_{Tz} + w)\rho g = \rho \frac{d}{dt}[(l_{Tz} + w)w'] - \rho \cdot (w')^2 + \frac{\rho}{4r_r}[(l_{Tz} + w)\,\lambda_r](w')^2 \mathrm{sgn}(V), \tag{15}$$

where p_{Tz} is the pressure measured by the transducer in the riser pipe and the last term on the right-hand side accounts for major frictional losses with λ_r defined as in Appendix B. Assuming negligible major frictional losses and a uniform velocity profile across the control surface at the transducer, the head measured by the transducer can be written in terms of deviation from static head ($h_{Tz} = p_{Tz}/(\rho g) - l_{Tz}$):

$$h_{Tz} = w + (l_{Tz} + w) \cdot w''/g. \tag{16}$$

The head h_{Tz} measured by the transducer differs from $w(t)$ by a term that is proportional to the product of the water level acceleration and the length of the water column above the pressure transducer ($l_{Tz} + w$). A similar equation was obtained by *Springer* [1991]. The dimensionless head response of the transducer in the riser pipe $\overline{h}_{Tz} = h_{Tz}/w_0$ is as follows:

$$\overline{h}_{Tz} = \overline{w} + (l_{Tz} + \overline{w}w_0)\overline{w}''/L_e. \tag{17}$$

[27] Using analytical expressions for w, w', and w'' from (16) and (17), transducer responses $h_{Tz}(t)$ were simulated for three depths of transducer placement l_{Tz} and are shown in Figure 4 with the h_{Tz} normalized by the initial displacement. Again, these head responses display a shift in phase and magnitude.

[28] An important feature present in the field data (Figure 2) but absent in the theoretical responses (Figure 4) are the pressure fluctuations at early times. These fluctuations, which appear to decrease in magnitude as the transducer is positioned at greater depths in the water column, are a direct consequence of the pneumatic method of initiating the slug test (see Appendix A). Previously, such fluctuations were either not observed due to insufficient recording frequency [*Zlotnik and McGuire*, 1998b] or attributed to noninstantaneous test initiation [*Butler et al.*, 1996, Figure 6]. Note that compressibility of the water attenuates the fluctuations with depth, and for the transducer at the screened section this "noise" is absent.

[29] As shown in Figure 4, the pressure response recorded by a transducer positioned in the water column (h_{Ts} or h_{Tz}) differs in phase and magnitude from the water level response $w(t)$. Indeed these differences must, by definition of potential flow, persist throughout the duration of the test. In addition, the largest displacement recorded by the transducer ($h_{\max} = \overline{h}_{\max} \cdot w_0$) is negatively correlated with the depth of the transducer, can be significantly less than the magnitude of the actual initial displacement w_0, and does not necessarily occur at the start of the test ($t = 0$).

[30] The experimental and simulated responses of Figures 2a and 4 show that the same water level dynamics can yield different transducer-measured head responses. Therefore analysis of transducer-measured head responses with conventional

type curves of water level response (i.e., hydrostatic interpretation) may be inappropriate if the transducer is positioned a distance below the static water level. For those conditions we recommend the dynamic interpretation using type curves of head response for the specific depth of transducer placement. This general approach is applicable to all types of slug tests that involve large acceleration of the water column. We evaluate the consequences of the hydrostatic interpretation in section 5.

4. Field Experiments

[31] The field component of this study was conducted at the Management Systems Evaluation Area (MSEA) research site near Shelton, Nebraska. It consisted of (1) installing two fully penetrating test wells with long screen lengths, (2) performing MLSTs at discrete intervals along the screened sections of both wells, and (3) performing an alternative hydraulic test, the dipole-flow test (DFT), to establish baseline profiles of K_r [*Zlotnik and Zurbuchen*, 1998; *Zlotnik et al.*, 2001].

4.1. Site Description

[32] The MSEA site is located on an alluvial terrace within the Platte River Valley [*Zlotnik and McGuire*, 1998b; *Zlotnik and Zurbuchen*, 1998]. The site is underlain by a 14 m thick unconfined sand and gravel Pleistocene aquifer. The water table typically lies between 4 and 8 m below the surface. The lower aquifer boundary is comprised of a 3–7 m thick silt-clay layer.

[33] Two fully penetrating 0.1 m ID wells, wells 14 and 15, were installed at MSEA in 1998 using reverse rotary drilling with clean water as the drilling fluid. The wells were placed 9 m away from one another. Clean water was sufficient for borehole stabilization and avoided possible invasion by drilling mud. A small borehole annulus (2.5 cm) was achieved using a 0.16 m diameter drill bit and a 0.11 m OD well screen. The wells were screened from 2.4 to 17.7 m below land surface. Screen slot size was 0.5 mm, resulting in an open area of 8.5%. The wells were completed by allowing the unconsolidated aquifer sediments to collapse on the well screen and then were developed by pumping.

4.2. Multilevel Slug Test Instrumentation

[34] The MLST instrument used in this study was developed by *Zlotnik and McGuire* [1998b]. It includes the following elements: (1) a double-packer assembly (DPA) with a riser pipe to isolate a test section l_s, (2) a pneumatic water level depressor to lower the water level, and (3) an air pressure gauge (0–150 cm H_2O) to measure actual water level displacement before test initiation. The MLST dimensions are as follows: l_p = 30 cm, r_r = 2.5 cm, r_s = 5.1 cm, and r_p = 1.9 cm (Figure 1b). Transient pressure responses were measured using a Druck PTX-161D transducer (pressure range 2.07×10^5 Pa (0–30 psi)) and recorded with a Campbell Scientific CR10X Data Logger at frequencies of 8, 12, or 16 Hz, depending on the test.

[35] In this work, results for one spacer configuration (l_s = 0.62 m) are presented. Note that the length of the water column, and therefore major frictional losses, are dependent on the elevation of the DPA [*Melville et al.*, 1991]. Air release is practically instantaneous for this particular MLST setup (see Appendix A).

4.3. Field MLST Procedures

[36] MLSTs were conducted along the screened intervals of wells 14 and 15 at 0.3-m (1-foot) increments. At each position, five tests were performed sequentially using w_0 = 0.165, 0.265, 0.470, 0.876, and 1.511 m, as measured by the air pressure gauge. The pressure transducer was positioned at the base of the tested section in all cases. At elevations where the response was clearly overdamped, only three tests were performed (w_0 = 0.470, 0.876, and 1.511 m). In selecting the above sequences of w_0, it was assumed that additional well development did not occur. This assumption is considered reasonable given the extensive primary well development and previous DFTs performed in these wells [*Zurbuchen et al.*, 1998].

5. Estimating Horizontal Hydraulic Conductivity

[37] In this section we outline several algorithms for estimating K_r from a set of slug tests performed in a given test interval using one or more w_0. The estimation of K_r is based on minimizing an objective function that is a measure of the difference between the observed and the predicted head response. First, the general algorithm for the dynamic interpretation of transducer response, which considers the inertial effects of the water column above the transducer, is given. This algorithm is then compared with the traditional algorithm, which assumes the transducer response to be equivalent to the water level response. The data-preprocessing techniques of translation and truncation are defined in order to apply the traditional algorithm. Two forms of the objective function are investigated. The first, for individual optimization, considers each test individually, while the second, for group optimization, considers the set of tests simultaneously to estimate a single K_r.

5.1. General Algorithm

[38] We assume that J tests were performed at each depth using initial displacements $w_{0,j}$ where j = 1, 2,. . ., J; J is the number of the test. We use the notation $\overline{h}_{Ts}(\tau_i, w_{0,j}, K_r)$ for the theoretically computed transducer response in the well screen. Index i denotes the dimensionless time τ_i elapsed from the start of the test, where i = 1, 2,. . ., I, and I is the total number of head values collected by the pressure transducer. The notation $\overline{h}_{Ts,j,i} = h_{Ts,j,i}/w_{0,j}$ is used for the observed transducer-measured head that is obtained in the jth test at time i and normalized by initial displacement $w_{0,j}$.

[39] The general estimation algorithm consists of the following steps. The specific slug test model (L_e and A_l) and form of the shape factor P are chosen. The initial value problem of (12) and (13) is solved with an assumed K_r and known initial displacement $w_{0,j}$ to obtain $\overline{w}(\tau, w_{0,j}, K_r)$, $\overline{w}'$ and $\overline{w}''$. These functions are substituted into (14) or (17) to yield the dimensionless head response at the tested screen section $\overline{h}_{Ts}(\tau, w_{0,j}, K_r)$,or at a depth l_{Tz} in the riser pipe $\overline{h}_{Tz}(\tau, w_{0,j}, K_r)$, respectively. The dimensionless theoretical and field-measured transducer responses are compared, and the objective function is calculated. The process is repeated until the K_r that minimizes the objective function is found.

5.1.1. Dynamic versus hydrostatic interpretation of transducer response. [40] The preceding section described an estimation algorithm based on the dynamic interpretation of transducer-measured responses. However, virtually all of the previous studies have used a hydrostatic interpretation of transducer responses. The traditional hydrostatic interpretation assumes that a transducer positioned at any depth in the water column records the water level response $\overline{w}(\tau)$. Therefore estimation of K_r is based on matching the dimensionless

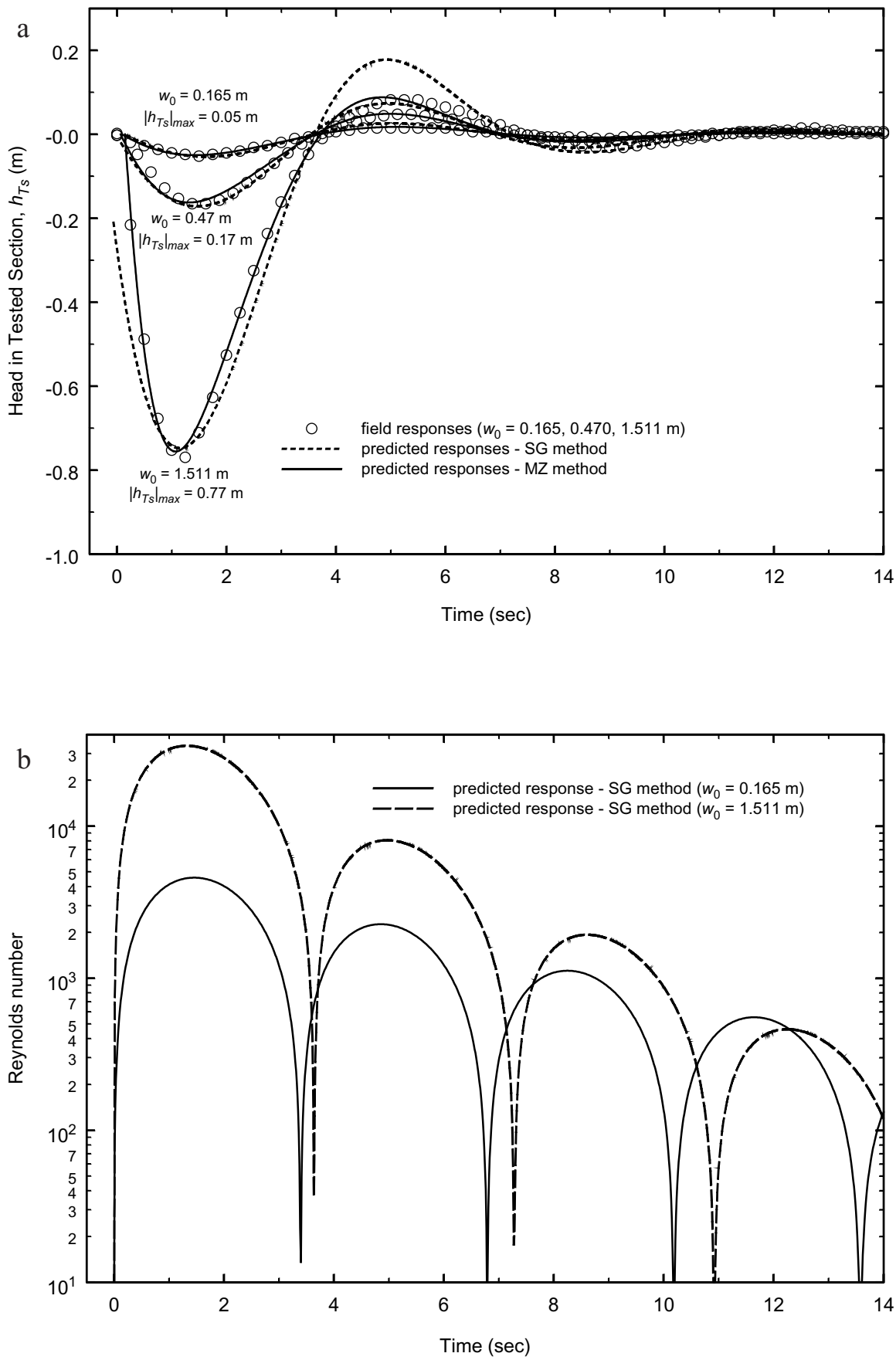

Figure 5. (a) Example results of individual optimization for subset of tests of Figure 3 using the dynamic interpretation of transducer-measured head. (b) Reynolds number for predicted responses from the Springer-Gelhar (SG) method.

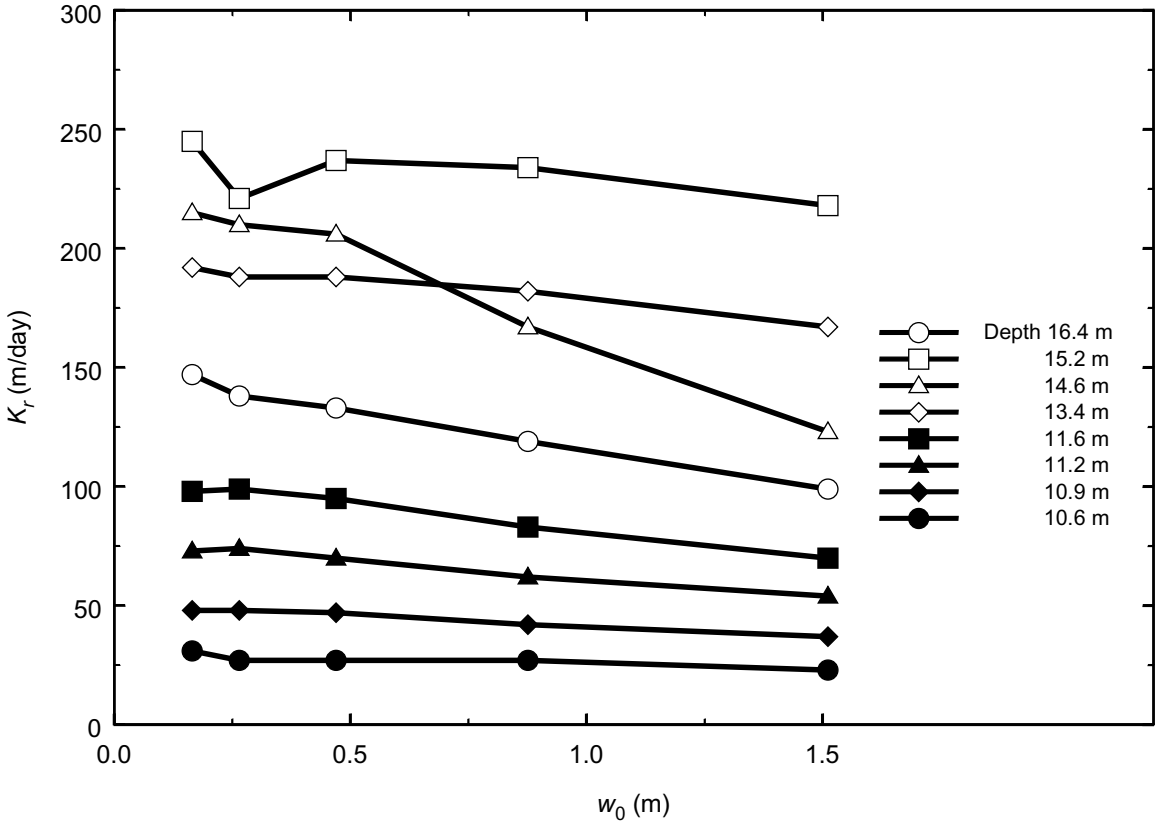

Figure 6. Dependence of K_r estimates (SG method) on w_0 for several test intervals in well 15.

simulated water level response $\overline{w}(\tau,\ w_{0,j},\ \mathrm{K_r})$ to the dimensionless field transducer response at either the well screen, $\overline{h}_{Ts,j,i}$, or at any given elevation in the riser pipe, $\overline{h}_{Tz,j,i} = h_{Tz,j,i}/w_{0,j}$. Unlike the dynamic interpretation this approach does not convert simulated water level $\overline{w}(\tau,\ w_{0,j},\ K_r)$ to head using (14) or (17).

5.1.2. Translation and truncation. [41] Limited "translation" of field data is traditionally used for the analysis of rapid oscillatory responses [*Kipp*, 1985; *Pandit and Miner*, 1986; *Butler*, 1997, p. 53]. Translation in time includes truncation of the early portion of the response and matching of the remaining part with simulated responses. The rationale behind translation is that hydraulic processes are complex and that instantaneous test initiation is technically difficult. *Butler* [1997] proposed to match the simulated water level response to the transducer-recorded head response starting from the first detectable peak or trough, where it was reasoned that the head derivative is zero. The motivation was "... to honor the condition that the initial velocity of the water column is zero..." [*Butler*, 1997, p. 161]. However, as follows from (17), the velocity of the water column in peaks or troughs of the transducer-recorded head response curve can deviate from zero. This discrepancy is illustrated in Figure 4, where the times of peak 1, peak 2, etc., do not coincide with the peaks of water level response. In highly permeable aquifers the truncated initial portion of the slug test data yields valuable information. It will be shown that when depth of transducer placement (l_{Ts} or l_{Tz}) is accounted for, translation is unnecessary.

5.1.3. Individual and group optimization and their objective functions. [42] Typically, multiple tests are performed at each isolated section using different initial displacements $w_{0,j}$. There are two approaches for estimating K_r. "Individual" optimization, the approach taken by *Springer and Gelhar* [1991] and *Zlotnik and McGuire* [1998b], yields a unique value of K_r for each individual test (i.e., one K_r estimate for each $w_{0,j}$). For individual optimization, K_r is estimated by minimizing the objective function of the sum of squared differences (SSD) $\mathrm{SSD}_j\ (K_r,\ w_{0,j})$ between the field data and the simulated response

$$\mathrm{SSD}_j\left(K_r, w_{0,j}\right) = \sum_{i=1}^{I} \left[\overline{h}_{Ts,\,j,i} - \overline{h}_{Ts}\left(\tau_i, w_{0,\,j}, K_r\right)\right]^2 \Delta\tau_i, \qquad \Delta\tau_i = \tau_{i+1} - \tau_i. \tag{18}$$

[43] "Group" optimization, advocated by *McElwee and Zenner* [1998], attempts to incorporate information from the entire set of tests and yields a single value of K_r for all tests (i.e., a single K_r estimate for all $w_{0,j}$). For group optimization, K_r is estimated by minimizing the sum of squared differences SSDG (K_r) over all tests performed at a particular location.

$$\mathrm{SSDG}\,(K_r) = \sum_{j=1}^{J} \mathrm{SSD}_j\left(K_r, w_{0,j}\right) \tag{19}$$

[44] The individual and group optimization objective functions given here are for a transducer positioned in the well screen. For responses recorded with the transducer in the riser pipe, $\overline{h}_{Ts,j,i}$ and

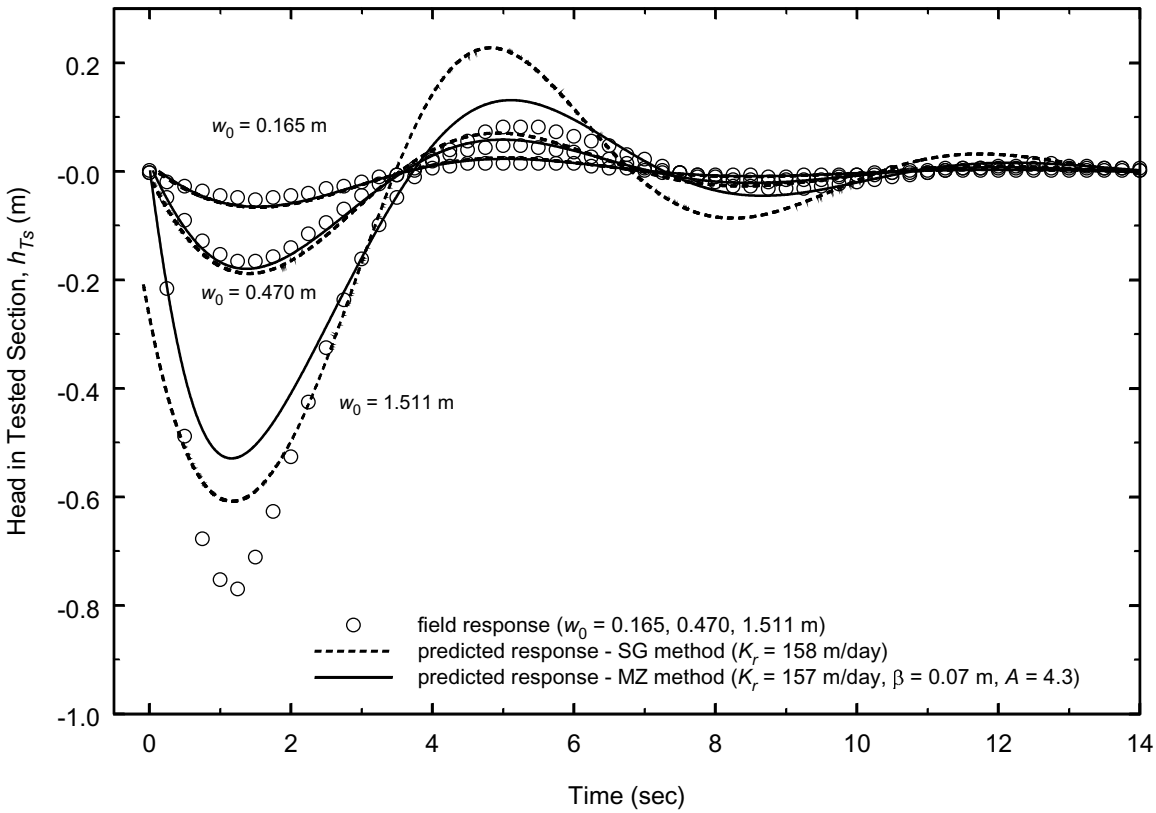

Figure 7. Example results of group optimization for subset of tests of Figure 3 using the dynamic interpretation of transducer-measured head.

$\overline{h}_{Ts}(\tau_i, w_{0,j}, K_r)$ in (18) and (19) are replaced by $\overline{h}_{Tz,j,i}$ and $\overline{h}_{Tz}(\tau_i, w_{0,j}, K_r)$, respectively.

5.2. Estimation of K_r Using the Dynamic Interpretation of Transducer Response

[45] The general algorithm for estimation of K_r outlined in section 5.1 was applied to each of the slug test models. Estimates of K_r were obtained by individual and group optimization using (18) and (19), respectively. Optimization of (18) and (19) for K_r in the SG and MSG models can be performed using any one-dimensional algorithm. Optimization of (18) and (19) for the three parameters A, L_e, and K_r in the MZ model was performed using the downhill simplex method [*Press et al.*, 1989].

[46] In the SG model, A_l was defined by (2), while we used (3) to define L_e in order to incorporate additional momentum changes due to contractions and expansions in our MLST system. For small initial displacements ($w_{0,j}/L_e \ll 1$) an analytical solution of (12) for $\overline{w}(\tau, w_{0,j}, K_r)$ is available [*Springer*, 1991; *Zlotnik and McGuire*, 1998a, equations (30)–(32)] and the calculation of $\overline{h}_{Ts}(\tau_i, w_{0,j}, K_r)$ by (14) is straightforward.

[47] The MSG model parameters L_e and A_l were defined by (3) and (4). In our analyses we assumed that the major loss component of A_l is negligible. The estimates of L_e and A_l introduce a weak nonlinearity into (12). Therefore the fourth-order Runga-Kutta method was used to calculate $\overline{w}(\tau_i, w_0, K_r)$ and $\overline{w}'(\tau_i, w_{0,j}, K_r)$. Values of $\overline{w}''(\tau_i, w_0, K_r)$ were obtained using backward differences. Head response at the screened interval $\overline{h}_{Ts}(\tau, w_{0,j}, K_r)$ was calculated by (14).

[48] In the MZ model, values of the empirical parameters L_e and A are not known a priori and therefore must be identified along with K_r. For each set of assigned parameters (A, L_e, and K_r), simulation of the nonlinear initial value problem of (12) was performed using the fourth-order Runga-Kutta method to calculate $\overline{w}(\tau, w_{0,j}, K_r, A, L_e)$ and $\overline{w}'(\tau, w_{0,j}, K_r, A, L_e)$. Values of $\overline{w}''(\tau, w_{0,j}, K_r, A, L_e)$ were obtained using backward differences. The head response at the base of the screened interval $\overline{h}_{Ts}(\tau, w_{0,j}, K_r, A, L_e)$ was then calculated with (14).

6. Discussion of Results

[49] A total of 762 MLSTs were performed at 68 locations in wells 14 and 15 at the MSEA site. On the basis of criteria for the occurrence of oscillations

$$K_r > K_c = \frac{r_r^2}{4 l_s P}\left(\frac{g}{L_e}\right)^{1/2} \tag{20}$$

developed using the SG model, where K_c is the critical hydraulic conductivity above which oscillations occur [*Zlotnik and McGuire*, 1998a, equation (33)], 47% of the responses were overdamped and 53% were underdamped. The MLST data sets were evaluated using the SG, MSG, and MZ models with both the traditional hydrostatic and the proposed dynamic interpretations. Individual and group optimizations were carried out for each model/interpretation method combination. Note that in this section all plots will be presented at 1/4 of the field-recorded frequency. The MLST results are compared to K_r profiles obtained with the single-borehole steady state DFT described by *Zlotnik and Zurbuchen* [1998]. This test has a simple interpretation, yields reliable and repeatable K_r profiles, and has a measurement scale similar to the

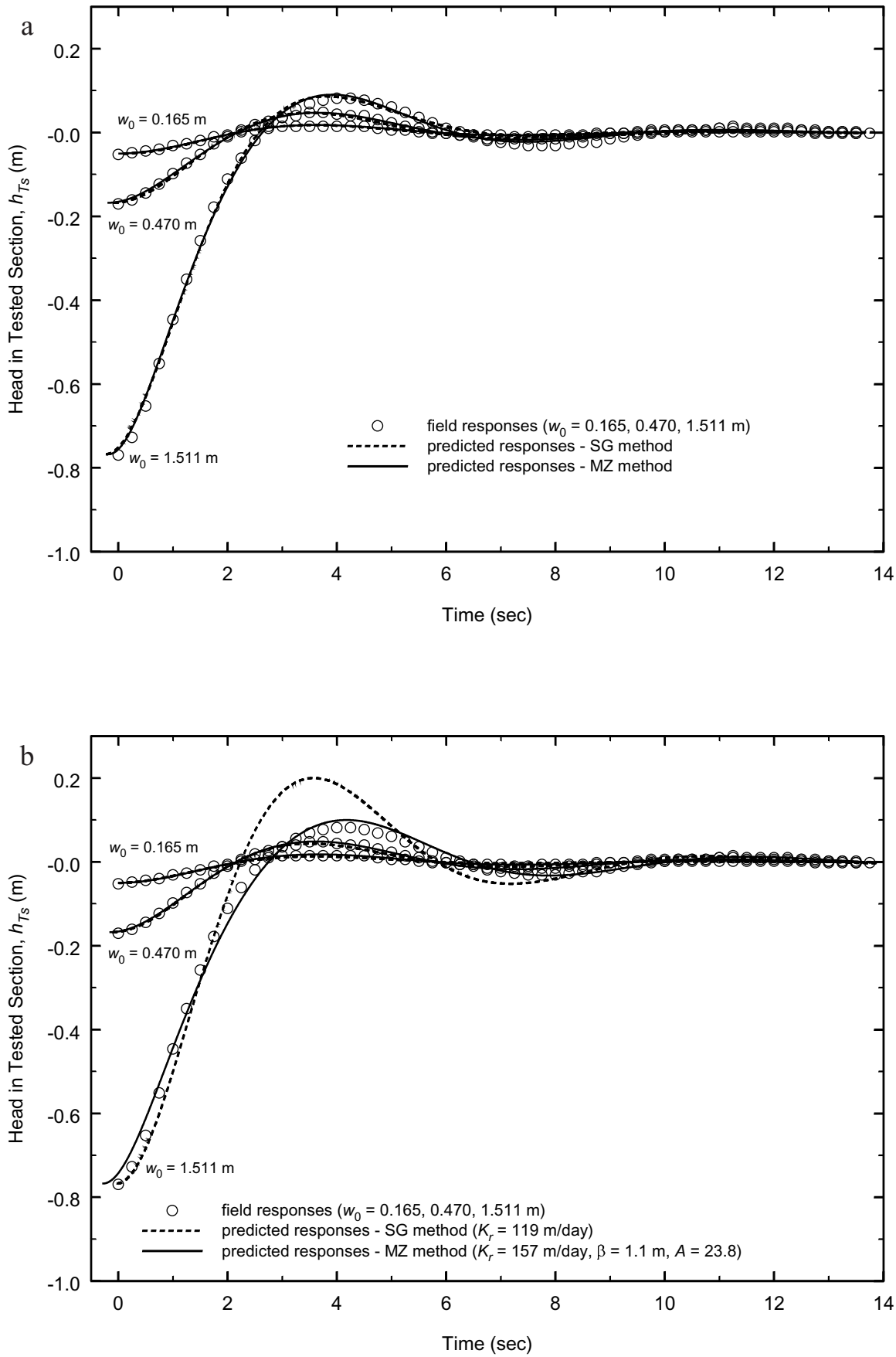

Figure 8. Example optimization results for subset of tests of Figure 3 using "translated" head response and the hydrostatic interpretation of transducer-measured head with (a) individual optimization and (b) group optimization.

Table 1. Dynamic Interpretation of Transducer Response

	SG Method		MZ Method			
$w_{0,j}$, m	K_r, m/d	SSD_j (SSDG)	K_r, m/d	A	β, m	SSD_j (SSDG)
			Individual Optimization			
0.165	214	0.20	195	26.9	0.6	0.02
0.265	203	0.16	189	14.5	0.6	0.02
0.470	181	0.17	167	9.2	0.0	0.01
0.876	147	0.20	136	5.2	−1.1	0.02
1.511	113	0.23	109	2.9	−2.3	0.02
			Group Optimization			
NA[a]	158	(1.54)	157	4.4	0.7	(1.07)

[a] NA, not applicable.

MLST [*Zlotnik et al.*, 2000]. Therefore we use it as a benchmark methodology to verify the results, to validate the proposed dynamic interpretation approach, and to highlight some caveats of the hydrostatic interpretation of the MLST.

6.1. Nonlinearity of MLST Responses

[50] The significance of nonlinear effects is dependent on the configuration and dimensions of the MSLT, the aquifer properties, and the magnitude of initial displacement [*McElwee and Zenner*, 1998]. The transition of MLST responses from the linear regime to one where nonlinear effects are present can be observed over the range of w_0 used in this study. Figure 3 displayed a set of oscillatory field responses (w_0 = 0.165, 0.265, 0.470, 0.876, and 1.511 m) normalized by their respective w_0. The similarity of normalized head responses for the two smallest initial displacements (w_0 = 0.165 and 0.265 m) suggests approximately linear behavior and the validity of linear slug test models [*Butler*, 1997, p. 167]. Responses from larger initial displacements (w_0 = 0.470, 0.876, and 1.511 m) do not coincide with one another; the amplitudes of the first peak differ by ∼60% and indicate the presence of nonlinear processes.

[51] These observations indicate that in highly permeable aquifers, multiple tests with a range of w_0 should be performed at every location in order to achieve a minimum of two responses that coincide. This will demonstrate the insignificant effect of frictional losses and appropriateness of a linear model for analysis of the responses [*Butler et al.*, 1996]. Such procedures can minimize the influence of the slug test configuration on the parameter estimates. In our program of MLSTs, linear behavior was consistently observed for tests using w_0 = 0.165 and 0.265 m.

6.2. Comparison of Various Models Using Dynamic Interpretation

6.2.1. Individual optimization. [52] The set of MLST responses displayed in Figure 3 is used to illustrate the individual optimization of parameters (18) for tests in which the dynamic interpretation of transducer response has been applied (14). The best fit theoretical pressure responses h_{Ts} from the linear SG and nonlinear MZ models for initial displacements w_0 = 0.165, 0.470, and 1.511 m are displayed in Figure 5a with parameter estimates given in Table 1. Results for the MSG model are not distinguishable from those of the SG model and thus are not displayed.

[53] The linear SG model fits the phase and magnitude of the field responses $h_{Ts,j}$ fairly well over the first half-period for all initial displacements. Although the deviation becomes larger for intermediate times, the relative deviation is similar for all displacements, as confirmed by the SSD_j values in Table 1. Using the three optimization parameters K_r, L_e (= L + β), and A, the MZ model predicts the field responses uniformly better throughout all the tests. Values of SSD_j from (18) are given in Table 1. The fit of the three-parameter MZ model is dramatically better than the one-parameter SG model for the entire range of w_0.

[54] Parameter estimates in Table 1 indicate that for a given w_0, estimates of K_r from the two models are within 10% of one another, with the SG model giving the higher K_r estimate. Both models yield similar estimates for small w_0 (≤0.30 m) but exhibit a negative correlation between w_0 and K_r for $w_0 \geq$ 0.47 m. Over the entire range of w_0, K_r from the SG and MZ models decreases by a factor of ≈2. Similar trends were observed by *McElwee and Zenner* [1998] in their applications of the SG model. Parameter A in the MZ model decreases by an order of magnitude, and β shifts from 0.6 to −2.3. These results appear contrary to the conjecture of *McElwee and Zenner* [1998], who suggested that a unique set of constant coefficients (K_r, A, and β) could adequately describe the MLST response for any w_0. Although A differs by almost a factor of 2 for the linear responses (w_0 = 0.165 and 0.265 m), β does not change.

[55] *McElwee and Zenner* [1998] recognized that the coefficient A, which accounts for major and minor frictional losses, could vary during a test, although they assumed it to be constant in their model. In order to evaluate this assumption, the Reynolds number Re based on the instantaneous absolute velocity in the riser pipe was calculated for the MLSTs with w_0 = 0.165 and 1.511 m and was plotted in Figure 5b. For w_0 = 1.511 m, Re varies by >1 order of magnitude (1000−34,000) over the first half-period, the Darcy friction factor λ (for smooth pipes and assuming transition to

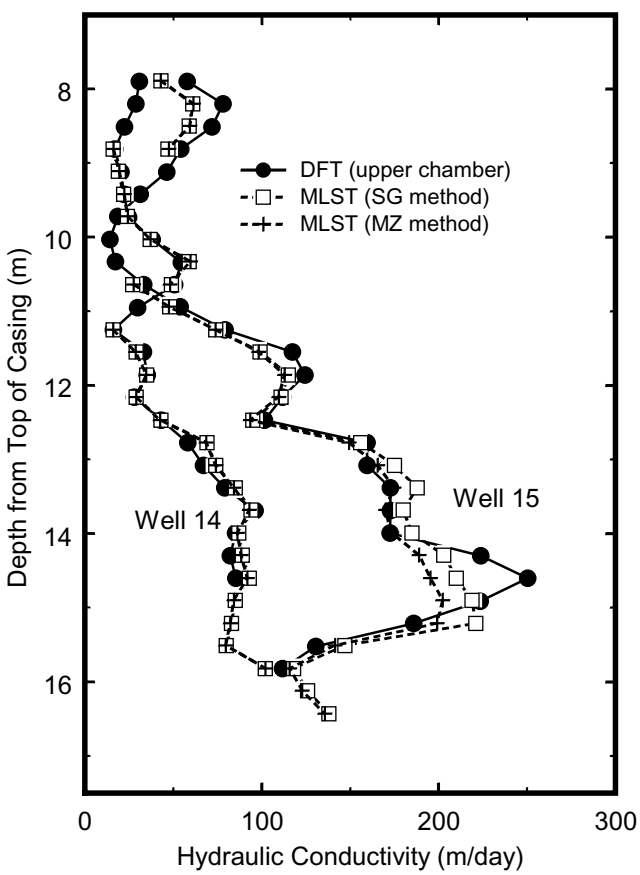

Figure 9. K_r profiles from the dipole-flow test and MLST for wells 14 and 15.

Table 2. Hydrostatic Interpretation of Transducer Response With Translation

			SG Method		MZ Method			
Actual $w_{0,j}$[a], m	$w_{0,}$[b] m	Time to Peak 1, s	K_r, m/d	SSD_j (SSDG)	K_r, m/d	A	β, m	SSD_j (SSDG)
			Individual Optimization					
0.165	0.05	1.5	150	0.30	148	5.4	1.3	0.24
0.265	0.08	1.6	147	0.25	164	−1.0	1.5	0.10
0.470	0.17	1.4	125	0.12	160	5.4	1.3	0.03
0.876	0.37	1.4	101	0.07	165	7.7	1.1	0.02
1.511	0.77	1.3	82	0.05	129	18.1	−1.8	0.03
			Group Optimization					
			119	(2.55)	157	23.8	1.1	(0.50)

[a] Pressure gauge.
[b] Peak 1, transducer response.

turbulent flow at $Re = 2000$) varies by a factor of >2 ($0.064 \geq \lambda \geq 0.023$), and the flow regime spans from laminar to turbulent flow regimes [*Fox and McDonald*, 1992, p. 350]. Even for $w_0 = 0.165$, where Re varies only by a factor of 4 (1000–4300), the Darcy friction factor varies significantly ($0.064 \geq \lambda \geq 0.015$) if we assume that the flow remains laminar [*Letelier and Leutheusser*, 1976]. Since A is strongly dependent on the Darcy friction factor, we conclude that assuming A is constant is often an oversimplification of the physical processes occurring during a slug test in a highly permeable aquifer.

[56] K_r estimates from the SG and MZ models with the dynamic interpretation are similar for the linear MLST responses ($w_0 \leq 0.265$ m), and we consider these estimates to be representative of the portion of the aquifer adjacent to the tested interval. The small w_0 minimized the magnitude of the quadratic nonlinear $A \cdot (w')^2$ term in (12). The negative correlation between K_r and w_0, for $w_0 \geq 0.470$ m, was consistent throughout the range of K_r found in this study. Figure 6 displays K_r (analyzed using the SG model with the dynamic interpretation) versus w_0 for MLSTs performed at eight different elevations within well 15. Figure 6 illustrates that there is typically a relative difference of 0–50% between the minimum and maximum estimated K_r for a given MLST configuration. For MLSTs performed with $w_0 \geq 0.470$ this relative difference is positively correlated with K_r, and w_0 and is due to the presence of nonlinear processes. The irregularity in the slope of the correlation for the MLST performed at depth 14.6 m may be an artifact of nonlinear processes, experimental error, or the optimization algorithm used to obtain K_r. For ~80% of the elevations tested in well 15 the relative difference in K_r estimates from the linear MLST responses (w_0 = 0.165 and 0.265 m) is ≤7%. However, at a few elevations the difference was as large as 15% and can be attributed to experimental error associated with the air pressure gauge used to calculate w_0, which increases with smaller w_0. Similar trends of K_r and w_0 were observed for the MZ model.

6.2.2. Group optimization. [57] *McElwee and Zenner* [1998] suggested that the dependence of K_r on w_0 found with previous models is an artifact of incomplete incorporation of nonlinear processes. They proposed that the MZ model be used to predict responses for a wide range of w_0 with a unique set of parameters (K_r, β, and A). To evaluate this hypothesis, the MLST field data from Figure 3 were reprocessed using group optimization (19) for both the SG and MZ models. Results are displayed in Figure 7 and parameter estimates are given in Table 1.

[58] The SG and MZ models yield practically the same K_r estimate, which lies in the middle of the range of estimates from the individual optimization. This is expected because group optimization applies equal weight to each normalized response. For the MZ model, parameter estimates of β and A are on the order of the estimates obtained from the individual optimization. However, Figure 7 illustrates a lack of universal fit for both models, which contrasts the conjecture of *McElwee and Zenner* [1998] concerning the existence of a unique set of parameters for their model. The reason is twofold. First, *McElwee and Zenner* [1998, Figure 6] presented analyses of only slightly oscillatory responses, which displayed both underdamped and overdamped characteristics, depending on $w_{0,j}$. Second, $w_{0,j}$ varied by a factor of < 4 in the tests they describe. In our tests, $w_{0,j}$ varied by almost 1 order of magnitude, and responses were significantly underdamped. For our MLST field data, which exhibited both linear and nonlinear behavior over the range of w_0, assuming a single set of parameters would be a significant simplification of the hydraulic processes during the slug test because A cannot be set to zero (SG model) or represented as a constant (MZ model) over the entire w_0 range.

6.3. Comparison of Various Models Using the Hydrostatic Interpretation

[59] The hydrostatic interpretation is commonly applied to analyze slug test data collected using transducers [*Butler*, 1997]. The field data from Figure 3 are used to evaluate this technique for tests in highly permeable aquifers. It is apparent that the transducer-measured responses do not resemble the typical types of *van der Kamp* [1976] or *Kipp* [1985] curves in that $|h_{Ts}|_{max}$ does not occur at test initiation. Therefore to select the initial displacement and starting time for the test, we resort to the preprocessing procedure of translation [*Pandit and Miner*, 1986]: (a) the early time portion of the response prior to peak 1 (see Figure 4) is truncated from the response record, (b) the displacement at peak 1 $|h_{Ts}|$ is taken as w_0, and (c) the response is translated along the time axis and assumed to start at this peak ($t = t_{peak\ 1} = 0$). For this configuration of the MLST, with the transducer at a significant depth below the static water level, this preprocessing is almost entirely objective since there is little "noise" near the first peak.

[60] Individual and group optimizations of the translated data from Figure 3 were performed and results are displayed in Figures 8a and 8b, respectively, with parameter estimates given in Table 2. Predicted water level responses from both models with individual optimization fit the transducer pressure response well. However,

comparison of Table 1 with Table 2 indicates that the SG model with the hydrostatic interpretation underestimates K_r, even in the range of linear responses ($w_0 \leq 0.265$ m), by almost 30% when compared to the dynamic interpretation. As in the dynamic interpretation, K_r from the SG model is negatively correlated with w_0. The MZ model also underestimates K_r, but estimates are more consistent over the range of w_0.

[61] For group optimization, water level responses predicted by the MZ model match the field transducer responses well. There is only slight deviation for $w_0 = 1.511$ m. Water level responses predicted by the SG model match field data well for $w_0 \leq 0.470$ m but deviate for $w_0 = 1.511$ m. The SG model gives $K_r = 119$ m/d, which lies near the lower end of the range for the individual optimization. Comparing parameter estimates with those from Table 1, we see that, for the MZ model, $K_r = 157$ m/d is consistent with the dynamic interpretation using group optimization, while the SG model estimate of K_r is significantly less. However, the consistency of the MZ is questionable since, using the same set of data, A is calculated to be >4 times that from the dynamic interpretation.

[62] The analyses presented in the previous paragraphs were for the worst-case scenario, the transducer in the test interval. The viability of the hydrostatic interpretation depends on transducer position. It is evident from these results that when the transducer is at a significant distance below the static water level, a traditional hydrostatic interpretation of transducer response leads to subjective preprocessing procedures, reduces the information in the data, and underestimates K_r for highly permeable aquifers [e.g., *Zlotnik and McGuire*, 1998b]. However, as the form of (17) makes clear, the hydrostatic interpretation may be adequate when transducers are placed close to the static water level. In formations of moderate to low permeability, where the velocity and acceleration of the water column are small, the hydrostatic interpretation is sufficient regardless of transducer depth.

6.4. Vertical Profiles of Horizontal Hydraulic Conductivity and Comparison With DFT

[63] Profiles of K_r were constructed using estimates obtained from the SG and MZ models with the dynamic interpretation and individual optimization ($w_0 = 0.265$ m). Figure 9 displays the MLST K_r profiles for wells 14 and 15. Results indicate that K_r is highly variable and increases with depth. K_r values estimated from the SG and MZ methods ranged from 16 to 219 m/d, with both methods yielding practically the same K_r for zones where $K_r < 150$ m/d. However, for zones of very high permeability ($K_r > 150$ m/d) the SG method systematically gives a higher estimate of K_r. Profiles of $K_{r,U}$ estimated from the upper chamber of the DFT [*Zlotnik et al.*, 2001], superimposed on Figure 9, compare well with K_r profiles from the MLST and display similar variability, trend, and magnitude. Only in two thin zones in well 15 (depths ~8.5 and ~15 m) is there notable difference (±25%) between the MLST and DFT results. We hypothesize that these differences are a result of either experimental error introduced by the air pressure gauge used to measure w_0, which could lead to either an overestimation or underestimation of K_r or short-circuiting flow between chambers during the DFT, which would lead to an overestimation of K_r.

[64] The K_r profiles suggest that in highly permeable heterogeneous aquifers the MLST and DFT give similar results for a wide range of K_r when: (1) MLST data are analyzed using either the SG, MSG, or MZ model with the dynamic interpretation of transducer measurements, (2) normalized MLST responses are independent of initial displacement, (3) DFT data are analyzed on the basis of individual chamber responses, (4) the vertical scale of the MLST test interval and DFT chambers are similar, and (5) the center of the MLST test interval and the center of the DFT chamber (upper or lower) coincide.

[65] The agreement between K_r estimates from the two different types of hydraulic tests must be considered excellent given the entirely different flow regimes of the two tests. The MLST involves horizontally dominated transient flow, while the DFT involves a recirculatory steady state flow regime. This excellent agreement between MLST and DFT K_r estimates also suggests that well completion procedures were effective.

7. Conclusions and Recommendations

[66] Three models for the analysis of slug tests in highly permeable formations (Springer-Gelhar (SG), modified Springer-Gelhar (MSG), and McElwee-Zenner (MZ)) were examined in this article. These models, originally formulated to predict water level response, combine momentum analysis of flow in the well and test equipment with a quasisteady model of water exchange between the well and the aquifer. However, these models did not address the commonly observed difference between the theoretical water level response and field data from a pressure transducer. Moreover, these models yield different estimates for K_r using the same data. This study provides an explanation for these phenomena and addresses both theoretical and technical issues concerning slug tests in highly permeable formations. In order to demonstrate the findings of this investigation, an extensive database of >750 MLSTs was collected at 68 positions within two wells in an alluvial aquifer. Specific conclusions and corresponding recommendations are formulated below.

1. The dynamic relationship between water level response and transducer-measured head that is derived from momentum conservation clearly shows that for slug tests in highly permeable aquifers the head response recorded by a submersed transducer cannot, in general, be translated to water level response using a hydrostatic relationship. The difference between the two relationships is approximately proportional to the product of the water level acceleration and depth of the transducer. A new dynamic interpretation for slug tests based on this relationship is presented and adapted to each of the slug test models (SG, MSG, and MZ). This interpretation quantitatively and qualitatively predicts the transient hydraulic head measured by the pressure transducer, including the initial portion of the slug test data that could not be explained previously and was commonly discarded from the analysis. K_r profiles obtained from the MLSTs using this approach are in excellent agreement with results obtained from the dipole-flow test despite dramatically different flow regimes invoked by the two methods. Therefore, in highly permeable aquifers, we recommend the dynamic interpretation of transducer-recorded head responses. Accurate measurements of w_0 are important for data interpretation using any slug test model, and the use of an air pressure transducer is recommended for pneumatically initiated tests [e.g., *Butler*, 1997, Figure 3.6].

2. Slug test responses can be nonlinear with respect to initial displacement w_0 in highly permeable aquifers. Our experiments support previous findings that it is possible to minimize this nonlinearity by reducing w_0 to a degree that major and minor head losses can virtually be neglected. In our field study the transition from a linear to a nonlinear dependence on w_0 occurred between initial displacements of 0.265 and 0.470 m. Generally, this transition point is dependent on test configuration and hydrogeological conditions. To obtain linear responses and locate the

transition point, we recommend performing slug tests with several (at least two) small displacements and evaluating test responses in their normalized form (h_{Tz}/w_0,) as suggested by *Butler et al.* [1996] and *McElwee and Zenner* [1998]. We also recommend that test configurations be designed to minimize head losses and to produce overdamped responses over the range of expected K_r according to criteria of (20).

3. Analysis of slug test responses affected by nonlinear processes confirmed the negative correlation between w_0 and K_r estimates. This negative correlation, which was found with all three models, is an indication of our current inability to adequately quantify all of the hydraulic processes occurring in the well and aquifer during a slug test. The three-parameter MZ model naturally produces better fits than the SG and MSG models but does not remove the negative correlation. Group optimization of several tests with various w_0 to find a unique set of parameters may not be valid unless all w_0 are within the range for linear responses. The fit of both linear and nonlinear responses may be improved by replacing the zero-storage (quasisteady) aquifer interaction model with one that considers aquifer storage [*Kipp*, 1985; *Stone and Clarke*, 1993].

4. In this study the SG model was found to be the simplest and, for practical purposes, the most useful for assessment of K_r values (as high as 224 m/d). The MZ model yields similar estimates but is more complex; however, it may have potential for use in aquifers of higher permeability. The MSG model, with its general functional form for frictional head losses, provides the most universal and flexible framework for future theoretical extensions to more permeable formations.

5. It is shown that the role of airflow in these pneumatically initiated slug tests is limited. For more conductive aquifers this factor should be evaluated using the more general model of (1) that includes air dynamics in the system.

6. The traditional hydrostatic interpretation of the slug test consistently underestimates K_r in the underdamped regime. The ad hoc preprocessing procedure of translation violates the initial condition of zero water level velocity at the peak or trough, i.e., the zero value of the time derivative of the head response is not equivalent to the zero value of the time derivative of the water level. The hydrostatic interpretation with translation can be adequate, for practical purposes, in moderately to highly permeable formations where water column acceleration is not large. However, the obtained K_r values should be verified using the dynamic interpretation.

Appendix A: Air Release for Pneumatic Slug Tests

[67] In highly permeable aquifers, where test initiation becomes an important factor, the pneumatic method introduced by *Prosser* [1981] is commonly used [e.g., *Butler*, 1997]. This approach involves placing an airtight seal on top of the riser pipe/casing. Using a compressor or pressurized gas cylinder, the water level in the well is depressed to a certain depth by pressurizing the air column above the water level. The increased pressure, measured by an air pressure gauge or transducer, is maintained until the aquifer reaches steady state. The test is initiated by quickly releasing the pressurized air through a valve. Although this release is assumed to be instantaneous ($p_{\text{air}}(t) = 0$), in practice, the evacuation time depends on release valve size, pressurized section geometry, and initial pressure. To our knowledge this factor has not been accurately documented beyond some initial work by *Prosser* [1981] that showed air escape times of <1 s from a pipe 5.1 cm in diameter but of undefined length.

[68] The dynamic air pressure release of the MLST instrument used in this study has been explored in a series of experiments in which the riser pipe radius was $r_r = 2.5$ cm and the length of the pressurized air column was approximately $l_a \approx 7.5$ m [*Zlotnik et al.*, 1997]. Figures A1a and A1b show the dynamics of the head in the water column and the air pressure for an overdamped and underdamped MLST response, respectively. Each set of responses was collected by sequentially performing two identical MLSTs using a 100-Hz data acquisition system, with the pressure transducer positioned at two different locations: 0.5 m above the static water level to record $p_{\text{air}}(t)$ and $l_{Tz} \approx 3$ m below the static water table to record $h_{Ts}(t)$. The air pressure response exhibits high-frequency pulsations of rapidly decreasing magnitude.

[69] Two features are apparent from these figures. The first feature is that the actual initial water level displacements (w_0 recorded by the air pressure gauge) differ from the maximum water level displacements ($|h_{Ts}|_{\max}$) recorded by the transducer. This discrepancy can be partially explained by the second feature, overpressure ($p_{\text{air}}(t) > 0$) on the water column [*Prosser*, 1981], which exhibits decreasing magnitude of pulsations of frequency $f \approx 10.5$ Hz. The pulsation follows that predicted by acoustic theory for air in a pipe of length l_a, which is closed on one end. On the basis of the speed of sound in air ($C = 340$ m/s at 15°C [*Fox and McDonald*, 1992]) and the length of the air-filled section of the MLST instrument ($l_a \approx 7.5$ m) the theory predicts a pressure frequency of $f = C/(4l_a) = 11.3$ Hz [*Milne-Thomson*, 1960].

[70] It is apparent that the period of air evacuation for this MLST configuration is much shorter than the duration of the first cycle of head response in the water column $h_{Ts}(t)$. Although the air evacuation plays some minor role in distorting the initial oscillatory cycle of the drawdown recovery, its magnitude is small, and $p_{\text{air}} \approx 0$ is a good approximation of the air dynamics of the system. Generally, it would be good practice to test each MLST system for this characteristic time by synchronous measurements of air and water pressure with data acquisition frequency higher than $f = C/(4l_a)$.

Appendix B: Calculating Major and Minor Losses in the MSG Model

[71] The major loss coefficient can be written as

$$\psi(w, V) = \frac{1}{4r_r}\left[(l_r + w)\,\lambda_r(V) + \frac{r_r^5}{r_p^5} l_p\;\lambda_p\left(\frac{r_r^2}{r_p^2}V\right)\right]\text{sgn}(V). \tag{B1}$$

The $\lambda_r(V)$ and $\lambda_p(r_r^2 V/r_p^2)$ coefficients are Darcy friction factors for flow in the riser pipe and packer pipe, respectively. The $\lambda_i (i = r$ or $p)$ coefficient can be defined on the basis of instantaneous pipe velocity V as $\lambda_i = 64/Re$ for laminar flow ($Re \leq 2000$) and $\lambda_i = 0.316/Re^{1/4}$ for turbulent flow ($2000 < Re < 10^5$). Here $Re = |V|D/\nu$ is the Reynolds number calculated using the respective riser pipe or packer pipe diameter D, velocity V, and the kinematic viscosity ($\nu = 1.3 \times 10^{-6}$ m^2/s for 10°C). Under certain conditions, neglecting major frictional losses ($\psi \approx 0$) yields adequate description of the flow in the MLST [*van der Kamp*, 1976]. Note that major frictional losses are dependent on the elevation of the slug test assembly [*Melville et al.*, 1991].

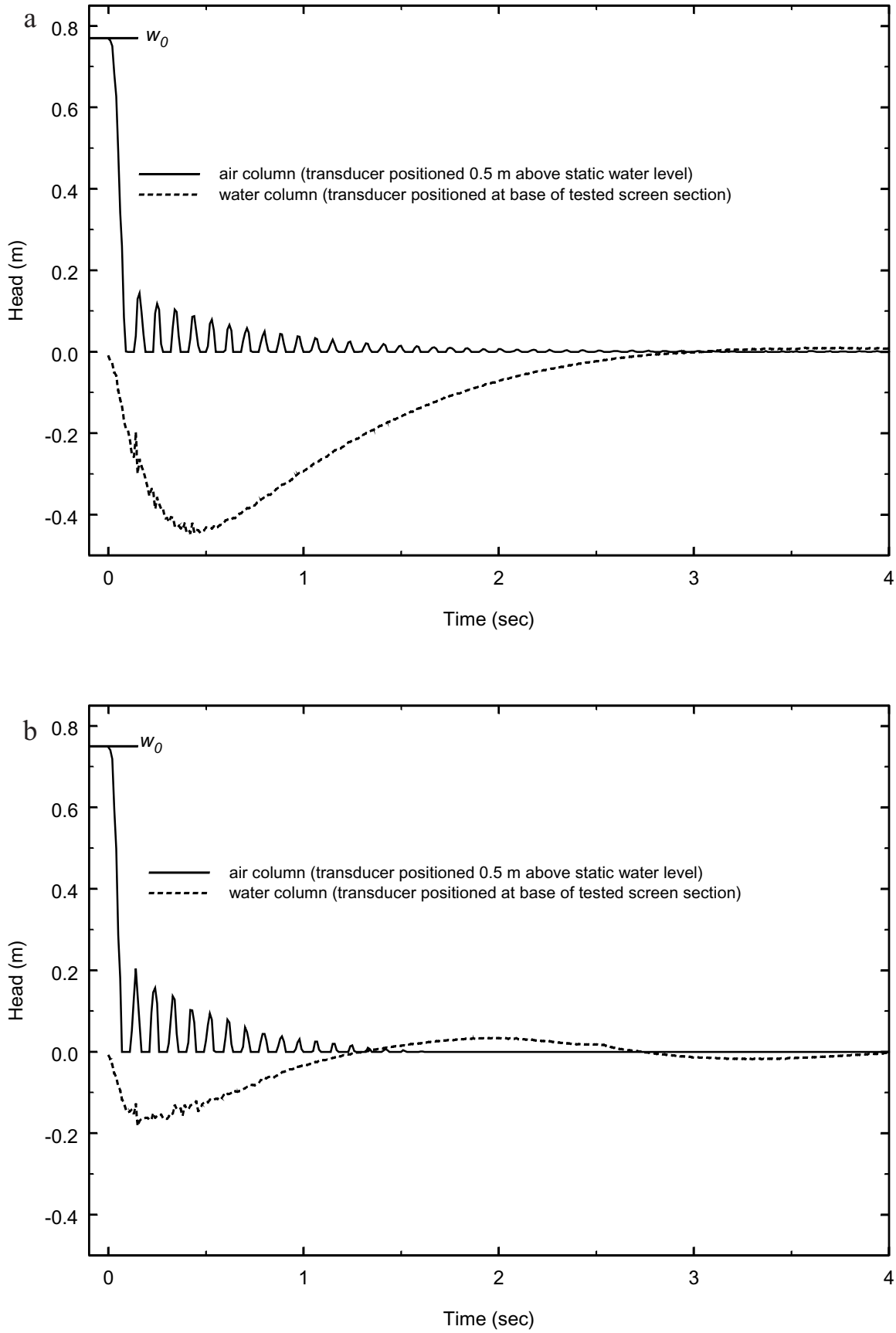

Figure A1. Pressure head responses in the water column and in the air column during an MLST (w_0 = 0.7 m) performed in well 15 at the Horkheimer Insel, Germany, field site. (a) Monotonic response from depth of 8.3 m. (b) Oscillatory response from depth of 7.7 m. MLST geometry is l_s = 0.65 m, l_p = 0.63 m, and $l_r \approx$ 1.3 and 1.9 m for Figures A1a and A1b, respectively, with r_s = 7.6 cm, r_p = 1.9 cm, and r_r = 2.5 cm.

[72] Minor loss coefficient ς can be written as

$$\varsigma(V) = 1 + \frac{r_r^4}{r_s^4} + \frac{r_r^4}{r_p^4}(k_{23} + k_{45})\mathrm{sgn}(V), \qquad \text{(B2)}$$

where k_{23} and k_{45} are defined as

$$k_{23} = \begin{cases} k_{23}^c = k^c(A_{23}), & V > 0 \\ k_{23}^e = k^e(A_{23}), & V < 0 \end{cases} \quad A_{23} = \left(\frac{r_p}{r_s}\right)^2 \qquad \text{(B3a)}$$

and

$$k_{45} = \begin{cases} k_{45}^e = k^e(A_{45}), & V > 0 \\ k_{45}^c = k^c(A_{45}), & V < 0 \end{cases} \quad A_{45} = \left(\frac{r_p}{r_s}\right)^2. \qquad \text{(B3b)}$$

Values of empirical contraction and expansion constants k_{23}^e, k_{23}^c, k_{45}^e, and k_{45}^c are available for steady state flow in some ranges of *Re* [e.g., *Fox and McDonald*, 1992].

[73] **Acknowledgments.** This work was supported by grants from the U.S. Geological Survey (1997–1998) and the Water Center of the University of Nebraska, Lincoln. We would like to thank Lorraine Olson (UNL, Department of Mechanical Engineering) for technical critique in the early stages of this work and Loren Neimach for providing access to the MSEA site. We are also grateful to D. Hart and to one anonymous reviewer for their constructive comments.

References

Bouwer, H., Discussion of Bouwer and Rice slug test review articles, *Ground Water*, *34*(1), 171, 1996.

Bouwer, H., and R. C. Rice, A slug test for determining hydraulic conductivity of unconfined aquifers with completely or partially penetrating wells, *Water Resour. Res.*, *12*(3), 423–428, 1976.

Bredehoeft, J. D., H. H. Cooper Jr., and I. S. Papadopulos, Inertial and storage effects in well-aquifer systems: An analog investigation, *Water Resour. Res.*, *2*(4), 697–707, 1966.

Brown, D. L., T. N. Narasimhan, and Z. Demir, An evaluation of the Bouwer and Rice method of slug test analysis, *Water Resour. Res.*, *31*(5), 1239–1246, 1995.

Burger, R. L., and K. Belitz, Measurement of anisotropic hydraulic conductivity in unconsolidated sands: A case study from a shoreface deposit, Oyster, Virginia, *Water Resour. Res.*, *33*(6), 1515–1522, 1997.

Butler, J. J. Jr., *The Design, Performance, and Analysis of Slug Tests*, Lewis, Boca Raton, Fla., 1997.

Butler, J. J. Jr., C. D. McElwee, and W. Liu, Improving the quality of parameter estimates obtained from slug tests, *Ground Water*, *34*(3), 480–490, 1996.

Corbett, P. W. M., J. L. Jensen, and K. S. Sorbie, A review of up-scaling and cross-scaling issues in core and log data interpretation and prediction, in *Core-Log Integration*, edited by P. K. Harvery and M. A. Lovell, *Geol. Soc. London, Spec. Publ. 136*, 1998.

Dagan, G., A note on packer, slug, and recovery tests in unconfined aquifers, *Water Resour. Res.*, *14*(5), 929–934, 1978.

Fox, R. W., and A. T. McDonald, *Introduction to Fluid Mechanics*, John Wiley, New York, 1992.

Hvorslev, M. J., Time lag and soil permeability in ground-water observations, *MS Bull. 36*, Waterw. Exp. Stn., Corps of Eng., U.S. Army, Vicksburg Miss., 1951.

Hyder, Z., and J. J. Butler Jr., Slug tests in unconfined formations: An assessment of the Bouwer and Rice technique, *Ground Water*, *33*(1), 16–22, 1995.

Kabala, Z. J., G. F. Pinder, and P. C. D. Milly, Analysis of well-aquifer response to a slug test, *Water Resour. Res.*, *21*(9), 1433–1436, 1985.

Kipp, K. L. Jr., Type curve analysis of inertial effects in the response of a well to a slug test, *Water Resour. Res.*, *21*(9), 1397–1408, 1985.

Letelier, M. F., and H. J. Leutheusser, Skin friction in unsteady laminar pipe flow, *J. Hydraul. Div. Am. Soc. Civ. Eng.*, *104*(6), 807–819, 1976.

McElwee, C. D., and M. A. Zenner, A nonlinear model for analysis of slug test data, *Water Resour. Res.*, *34*(1), 55–66, 1998.

Melville, J. G., F. J. Molz, O. Guven, and M. A. Widdowson, Multilevel slug tests with comparisons to tracer data, *Ground Water*, *29*(6), 897–907, 1991.

Milne-Thomson, L. M., *Theoretical Hydrodynamics*, MacMillan, Old Tappan, N.J., 1960.

Pandit, N. S., and R. F. Miner, Interpretation of slug test data, *Ground Water*, *24*(6), 743–749, 1986.

Press, W. H., B. P. Flannery, S. A. Teukolsky, and W. T. Vetterling, *Numerical Recipes (Fortran Version)*, Cambridge Univ. Press, New York, 1989.

Prosser, D. W., A method of performing response tests on highly permeable aquifers, *Ground Water*, *19*(6), 588–592, 1981.

Springer, R. K., Application of an improved slug test analysis to the large-scale characterizaiton of heterogeneity in a Cape Cod aquifer, M. S. thesis, Mass. Inst. of Technol., Cambridge, Mass. 1991.

Springer, R. K., and L. W. Gelhar, Characterization of large scale aquifer heterogeneity in glacial outwash by analysis of slug tests with oscillatory response, Cape Cod, Massachusetts, in *Toxic Substances Hydrology Program, Proceedings of the Technical Meeting, Monterey, California, March 11–15, 1991*, edited by G. Mallard and D. Aronson, *U.S. Geol. Surv. Water Res. Invest. Rep. 91–4034*, pp. 3–40, Reston, Va., 1991.

Stone, D. B., and G. K. C. Clarke, Estimation of subglacial hydraulic properties from induced changes in basal water pressure: A theoretical framework for borehole response tests, *J. Glaciol.*, *39*(132), 327–340, 1993.

Streltsova, T. D., *Well Testing in Heterogeneous Formations*, John Wiley, New York, 1988.

van der Kamp, G., Determining aquifer transmissivity by means of well response tests: The underdamped case, *Water Resour. Res.*, *12*(1), 71–77, 1976.

Van Rooy, D., A note on the computerized interpretation of slug test data, *Inst. Hydrodyn. Hydraulic Eng. Prog. Rep. 66*, Tech. Univ., Denmark, 1988.

Widdowson, M. A., F. J. Molz, and J. G. Melville, An analysis technique for multilevel and partially penetrating slug test data, *Ground Water*, *28*(6), 937–945, 1990.

Zlotnik, V. A., Interpretation of slug and packer tests in anisotropic aquifers, *Ground Water*, *32*(5), 761–766, 1994.

Zlotnik, V. A., and V. L. McGuire, Multi-level slug tests in highly permeable formations, 1, Modification of the Springer-Gelhar (SG) model, *J. Hydrol.*, *204*, 271–282, 1998a.

Zlotnik, V. A., and V. L. McGuire, Multi-level slug tests in highly permeable formations, 2, Hydraulic conductivity identification, method verification, and field applications, *J. Hydrol.*, *204*, 283–296, 1998b.

Zlotnik, V. A., and B. R. Zurbuchen, Dipole probe: Design and field applications of a single-borehole device for measurements of vertical variations of hydraulic conductivity, *Ground Water*, *36*(6), 884–893, 1998.

Zlotnik, V. A., B. R. Zurbuchen, and T. Ptak, Applicability of the dipole flow test (DFT) and multi-level slug test (MLST) in highly conductive sediments: Horkheimer Insel Site, Germany, *Eos Trans. AGU*, *77*(46), Fall Meet. Suppl., F192, 1997.

Zlotnik, V. A., B. R. Zurbuchen, T. Ptak, and G. Teutsch, Support volume and scale effect in hydraulic conductivity: Experimental aspects, in *Theory, Modeling, and Field Investigation in Hydrogeology: A Special Volume in Honor of Shlomo P. Neuman's 60th Birthday*, edited by D. Zhang and C. L. Winter, Geol. Soc. of Am., Boulder, Colo, 2000.

Zlotnik, V. Z., B. R. Zurbuchen, and T. Ptak, The steady-state dipole-flow tests for characterization of hydraulic conductivity statistics in a highly permeable aquifer: Horkheimer Insel Site, Germany, *Ground Water*, *39*(4), 504–516, 2001.

Zurbuchen, B. R., V. A. Zlotnik, J. J. Butler Jr., J. Healy, and T. Ptak, Steady-state dipole flow tests in sand and gravel aquifers: Summary of field results, *Geol. Soc. Am. Abstr. Programs*, *30*(7), A226, 1998.

J. J. Butler Jr., Kansas Geological Survey, University of Kansas, 1930 Constant Ave., Campus West, Lawrence, KS 66407, USA. (jbutler@pcmail.kgs.ukans.edu)

V. A. Zlotnik and B. R. Zurbuchen, Department of Geosciences, University of Nebraska, Lincoln, NE 68588, USA. (vzlotnik@unl.edu; brian.zurbuchen@ndeq.state.ne.us)